Available online at www.sciencedirect.com
SCIENCE DIRECT®

ELSEVIER

Physica D 212 (2005) 20–53

PHYSICA D

www.elsevier.com/locate/physd

Persistence and stability of discrete vortices in nonlinear Schrödinger lattices

D.E. Pelinovsky[a], P.G. Kevrekidis[b,*], D.J. Frantzeskakis[c]

[a] *Department of Mathematics, McMaster University, Hamilton, Ontario, Canada L8S 4K1*
[b] *Department of Mathematics, University of Massachusetts, Amherst, MA 01003-4515, USA*
[c] *Department of Physics, University of Athens, Panepistimiopolis, Zografos, Athens 15784, Greece*

Received 5 November 2004; received in revised form 9 September 2005; accepted 16 September 2005
Available online 2 November 2005
Communicated by J. Lega

Abstract

We study discrete vortices in the two-dimensional nonlinear Schrödinger lattice with small coupling between lattice nodes. The discrete vortices in the anti-continuum limit of zero coupling represent a finite set of excited nodes on a closed discrete contour with a non-zero charge. Using the Lyapunov–Schmidt reductions, we analyze continuation and termination of the discrete vortices for small coupling between lattice nodes. An example of a square discrete contour is considered that includes the vortex cell (also known as the off-site vortex). We classify families of symmetric and asymmetric discrete vortices that bifurcate from the anti-continuum limit. We predict analytically and confirm numerically the number of unstable eigenvalues associated with each family of such discrete vortices.

Keywords: Two-dimensional nonlinear Schrödinger lattice; Lyapunov–Schmidt reductions; Discrete solitons; Discrete vortices; Persistence analysis; Stability analysis

1. Introduction

Discrete systems and differential-difference equations have become topics of increasing physical and mathematical importance. The variety of physical applications where such models are relevant, and their significant differences from the mathematical theory of partial differential equations, contribute to the extensive recent interest in these topics. The applicability of such models extends to areas as diverse as nonlinear optics, atomic and soft

* Corresponding author.
E-mail address: kevrekid@math.umass.edu (P.G. Kevrekidis).

0167-2789/$ - see front matter
doi:10.1016/j.physd.2005.09.015

condensed-matter physics, as well as biophysics. Specific details and references can be found in our first paper [1] as well as in reviews [2–7].

The present work is devoted to the existence and stability of coherent structures in two-dimensional lattices, which include both discrete solitons [6,7] and discrete vortices [8,9] (see also the pioneering work of [2] and the works of [10,11] for Klein–Gordon lattices). These two-dimensional coherent structures have emerged recently in studies of photorefractive crystals in nonlinear optics [12,13] and droplets of optical lattices in Bose–Einstein condensates [14,15]. A significant boost to this subject was given by the experimental realization of two-dimensional photonic crystal lattices with periodic potentials based on the ideas of [12]. As a result, discrete solitons were observed in [16,17], while more complex structures such as dipoles, soliton trains and vector solitons were observed in [18–20].

Most recently, observations of discrete vortices were reported by two independent groups [21,22] where the fundamental vortices with topological charge *one* were experimentally created and detected in photorefractive crystals. Two main examples of charge-one discrete vortices include a *vortex cross* (an on-site centered vortex) and a *vortex cell* (an off-site centered vortex). These structures were also recently predicted in a continuous two-dimensional model with the periodic potential [23].

These discoveries have stimulated further theoretical work and numerical computations. Thus, while in [9], discrete vortices of charge *two* were shown to be unstable, recently in [24] discrete vortices of charge *three* were found to be stable. Based on the theoretical predictions of [24], further experiments on localized structures were undertaken to unveil other interesting structures, such as the discrete soliton necklace [25]. The discrete vortices have been also extended to three-dimensional discrete and periodic continuum models [26–28]. Furthermore, asymmetric vortices have been recently predicted in the two-dimensional lattices in [29].

The above activity clearly signals the importance and experimental relevance of discrete solitons and vortices in two-dimensional discrete lattices. However, most of the above-mentioned works are predominantly of experimental or numerical nature, while the mathematical theory of existence and stability of discrete localized structures has not been developed to a similar extent. The only analytical method which was developed so far relied on computations of effective action functionals (see Sections 3.2, 3.3 in [2]). It was applied to the one-dimensional discrete NLS lattice in [30] and later extended to the computations of effective Hamiltonians [31].

The aim of the present paper is to develop a categorization of discrete solitons and vortices in the discrete two-dimensional nonlinear Schrödinger (NLS) equations. We start from a well-understood limit [32] (the so-called anti-continuum case of zero coupling between the lattice nodes) and examine the persistence of the limiting solutions for small coupling by means of the Lyapunov–Schmidt theory. This method allows us to discuss persistence and stability of the localized structures by analyzing finite-dimensional linear eigenvalue problems. The theoretical predictions agree well with full numerical computations of the discrete two-dimensional NLS equation. The method of Lyapunov–Schmidt reductions, which we employ in this paper, generalizes the pioneering method of [32], which is based on the implicit function theorem. Very similar results on the existence and stability of two-dimensional discrete vortices were obtained independently in [33] for a triangular lattice of weakly coupled Hamiltonian oscillators. The method of [33] relies on the averaging theory of effective Hamiltonians, which determine the dynamics near the discrete localized mode using Taylor series approximations.

Our main results are summarized for the simplest localized structures in Table 1. These results corroborate and extend the previously reported experimental and numerical findings. We quantify the stability of the charge-one vortex in accordance with [9,21–23], the instability of the charge-two vortex in accordance with [9,24] and the stability of the charge-three vortex in accordance with [24]. We further demonstrate the instability of all asymmetric vortices, which persist in the two-dimensional discrete lattice. Furthermore, our results can be used to extract the spectral stability of the dipole mode considered in [18] and of the soliton necklace of [25].

The paper is structured as follows. Abstract results on the existence of discrete solitons and vortices are derived in Section 2. Persistence of localized modes for a particular square discrete contour is considered in Section 3. Stability of the persistent solutions is addressed in Section 4. Analytical results are compared to numerical computations in Section 5. Section 6 concludes the paper.

Table 1
The numbers of eigenvalues of linearized energy and the linearized stability problem, associated with discrete vortices in the two-dimensional NLS lattice with small coupling between lattice nodes

Contour S_M	Vortex of charge L	Linearized energy H	Stable and unstable eigenvalues
$M = 1$	symmetric $L = 1$	$n(H) = 5$, $p(H) = 2$	$N_r = 0$, $N_i^+ = 1$, $N_i^- = 2$, $N_c = 0$
$M = 2$	symmetric $L = 1$	$n(H) = 8$, $p(H) = 7$	$N_r = 1$, $N_i^+ = 0$, $N_i^- = 0$, $N_c = 3$
$M = 2$	symmetric $L = 2$	$n(H) = 10$, $p(H) = 5$	$N_r = 1$, $N_i^+ = 2$, $N_i^- = 4$, $N_c = 0$
$M = 2$	symmetric $L = 3$	$n(H) = 15$, $p(H) = 0$	$N_r = 0$, $N_i^+ = 0$, $N_i^- = 7$, $N_c = 0$
$M = 2$	asymmetric $L = 1$	$n(H) = 9$, $p(H) = 6$	$N_r = 6$, $N_i^+ = 0$, $N_i^- = 1$, $N_c = 0$
$M = 2$	asymmetric $L = 3$	$n(H) = 14$, $p(H) = 1$	$N_r = 1$, $N_i^+ = 0$, $N_i^- = 6$, $N_c = 0$

The numbers $n(H)$ and $p(H)$ stand for negative and small positive eigenvalues of H, such that $n(H) + p(H) = 8M - 1$. The numbers N_r, N_i^+, N_i^-, and N_c stand for eigenvalues of the linearized stability problem with $\mathrm{Re}(\lambda) > 0$, $\mathrm{Im}(\lambda) = 0$; $\mathrm{Re}(\lambda) = 0$, $0 < \mathrm{Im}(\lambda) \ll 1$ and positive Krein signature; $\mathrm{Re}(\lambda) = 0$, $0 < \mathrm{Im}(\lambda) \ll 1$ and negative Krein signature; and $\mathrm{Re}(\lambda) > 0$, $\mathrm{Im}(\lambda) > 0$ respectively, such that $2N_r + 2N_i^+ + 2N_i^- + 4N_c = 2(4M - 1)$. The negative index theory [1] implies that $N_r + 2N_i^- + 2N_c = n(H) - 1$, which is confirmed by the table data.

2. Existence of discrete vortices

We consider the discrete nonlinear Schrödinger (NLS) equation in two spatial dimensions [5]:

$$\mathrm{i}\dot{u}_{n,m} + \epsilon(u_{n+1,m} + u_{n-1,m} + u_{n,m+1} + u_{n,m-1} - 4u_{n,m}) + |u_{n,m}|^2 u_{n,m} = 0, \quad (2.1)$$

where $u_{n,m}(t) : \mathbb{R}_+ \to \mathbb{C}$, $(n, m) \in \mathbb{Z}^2$, and $\epsilon > 0$ is the inverse squared step size of the lattice. The discrete NLS equation (2.1) is a Hamiltonian system with the Hamiltonian function

$$H = \sum_{(n,m)\in\mathbb{Z}^2} \epsilon|u_{n+1,m} - u_{n,m}|^2 + \epsilon|u_{n,m+1} - u_{n,m}|^2 - \frac{1}{2}|u_{n,m}|^4. \quad (2.2)$$

Besides the conserved Hamiltonian (2.2), the discrete NLS equation conserves the squared l^2-norm, called the power:

$$Q = \sum_{(n,m)\in\mathbb{Z}^2} |u_{n,m}|^2. \quad (2.3)$$

The power conservation is related to the invariance of the discrete NLS equation (2.1) with respect to the gauge transformation:

$$u_{n,m}(t) \mapsto u_{n,m}(t)\mathrm{e}^{\mathrm{i}\theta_0}, \qquad \forall\theta_0 \in \mathbb{R}. \quad (2.4)$$

Time-periodic localized modes of the discrete NLS equation (2.1) take the form

$$u_{n,m}(t) = \phi_{n,m}\mathrm{e}^{\mathrm{i}(\mu-4\epsilon)t+\mathrm{i}\theta_0}, \qquad \phi_{n,m} \in \mathbb{C},\ (n, m) \in \mathbb{Z}^2, \quad (2.5)$$

where $\theta_0 \in \mathbb{R}$ and $\mu \in \mathbb{R}$ are parameters. Since localized modes in the focusing NLS lattice (2.1) with $\epsilon > 0$ may exist only for $\mu > 4\epsilon$ [4] and the parameter μ is scaled out by the scaling transformation,

$$\phi_{n,m} = \sqrt{\mu}\hat{\phi}_{n,m}, \qquad \epsilon = \mu\hat{\epsilon}, \quad (2.6)$$

the parameter $\mu > 0$ will henceforth be set as $\mu = 1$. In this case, the complex-valued $\phi_{n,m}$ solve the nonlinear difference equations on $(n, m) \in \mathbb{Z}^2$:

$$(1 - |\phi_{n,m}|^2)\phi_{n,m} = \epsilon\left(\phi_{n+1,m} + \phi_{n-1,m} + \phi_{n,m+1} + \phi_{n,m-1}\right). \quad (2.7)$$

As $\epsilon = 0$, the localized modes of the difference equations (2.7) are given by the limiting solution:

$$\phi^{(0)}_{n,m} = \begin{cases} e^{i\theta_{n,m}}, & (n,m) \in S, \\ 0, & (n,m) \in \mathbb{Z}^2 \setminus S, \end{cases} \tag{2.8}$$

where S is a finite set of nodes on the lattice $(n,m) \in \mathbb{Z}^2$ and $\theta_{n,m}$ are parameters for $(n,m) \in S$. Since θ_0 is arbitrary in the ansatz (2.5), we can set $\theta_{n_0,m_0} = 0$ for a particular node $(n_0, m_0) \in S$. Using this convention, we define two special types of localized modes, called discrete solitons and vortices.

Definition 2.1. The localized solution of the difference equations (2.7) with $\epsilon > 0$, that has all real-valued amplitudes $\phi_{n,m}$, $(n,m) \in \mathbb{Z}^2$, and satisfies the limit (2.8) with all $\theta_{n,m} = \{0, \pi\}$, $(n,m) \in S$, is called a discrete soliton.

Definition 2.2. Let S be a simple closed discrete contour on the plane $(n,m) \in \mathbb{Z}^2$. The localized solution of the difference equations (2.7) with $\epsilon > 0$, that has complex-valued $\phi_{n,m}$, $(n,m) \in \mathbb{Z}^2$, and satisfies the limit (2.8) with $\theta_{n,m} \in [0, 2\pi]$, $(n,m) \in S$, is called a discrete vortex.

Definition 2.3. Let S be a simple closed discrete contour on the plane $(n,m) \in \mathbb{Z}^2$ such that each node $(n,m) \in S$ has exactly two adjacent nodes in vertical or horizontal directions along S. Let $\Delta\theta_j$ be the phase difference between two successive nodes in the contour S, defined according to the enumeration $j = 1, 2, \dots, \dim(S)$, such that $|\Delta\theta_j| \le \pi$. If the phase differences $\Delta\theta_j$ are constant along S, the discrete vortex is called symmetric. Otherwise, it is called asymmetric. The total number of 2π phase shifts across the closed contour S is called the vortex charge.

In particular, we consider the square discrete contour $S = S_M$:

$$S_M = \{(1,1), (2,1), \dots, (M+1, 1), (M+1, 2), \dots, (M+1, M+1), \\ (M, M+1), \dots, (1, M+1), (1, M), \dots, (1, 2)\}, \tag{2.9}$$

where $\dim(S_M) = 4M$. According to Definition 2.3, the contour S_M for a fixed M could support symmetric and asymmetric vortices with some charge L. The simplest vortex is the symmetric charge-one vortex cell ($M = L = 1$: $\theta_{1,1} = 0$, $\theta_{2,1} = \frac{\pi}{2}$, $\theta_{2,2} = \pi$, $\theta_{1,2} = \frac{3\pi}{2}$) [9,23]. Although the main formalism of our paper is developed for any $M \ge 1$, we obtain a complete set of results on persistence and stability of discrete vortices only in the cases $M = 1, 2, 3$, which are of most physical interest. The contours S_M for $M = 1$ and $M = 2$ are shown in Fig. 1.

It follows from the general method [2,32] that the discrete solitons of the two-dimensional NLS lattice (2.7) (see Definition 2.1) can be continued to the domain $0 < \epsilon < \epsilon_0$ for some $\epsilon_0 > 0$. It is more complicated to find a configuration of $\theta_{n,m}$ for $(n,m) \in S$ that allows us to continue the discrete vortices (see Definition 2.2) for $\epsilon > 0$. The continuation of the discrete solitons and vortices is based on the Implicit Function Theorem and the Lyapunov–Schmidt Reduction Theorem [34,35]. Abstract results on the existence of such continuations are formulated and proved below, after the introduction of some relevant notation.

Let $\mathcal{O}(0)$ be a small neighborhood of $\epsilon = 0$ such that $\mathcal{O}(0) = (-\epsilon_0, \epsilon_0)$ for some $\epsilon_0 > 0$. Let $N = \dim(S)$ and $\mathcal{T}$ be the torus on $[0, 2\pi]^N$ such that $\theta_{n,m}$ for $(n,m) \in S$ form a vector $\boldsymbol{\theta} \in \mathcal{T}$. Let $\Omega = l^2(\mathbb{Z}^2, \mathbb{C})$ be the Hilbert space of square-summable complex-valued sequences $\{\phi_{n,m}\}_{(n,m)\in\mathbb{Z}^2}$, equipped with the inner product and the norm

$$(\mathbf{u}, \mathbf{v})_\Omega = \sum_{(n,m)\in\mathbb{Z}^2} \bar{u}_{n,m} v_{n,m}, \qquad \|\mathbf{u}\|^2_{l^2} = \sum_{(n,m)\in\mathbb{Z}^2} |u_{n,m}|^2 < \infty. \tag{2.10}$$

Let $\mathbf{u}$ denote an infinite-dimensional vector in Ω that consists of components $u_{n,m}$ for all $(n,m) \in \mathbb{Z}^2$.

Proposition 2.4. *There exists a unique (discrete soliton) solution of the difference equations (2.7) in the domain $\epsilon \in \mathcal{O}(0)$ that satisfies (i) $\phi_{n,m} \in \mathbb{R}$, $(n,m) \in \mathbb{Z}^2$ and (ii) $\lim_{\epsilon\to 0} \phi_{n,m} = \phi^{(0)}_{n,m}$, where $\phi^{(0)}_{n,m}$ is given by (2.8) with $\theta_{n,m} = \{0, \pi\}$, $(n,m) \in S$. The solution $\boldsymbol{\phi}(\epsilon)$ is analytic in $\epsilon \in \mathcal{O}(0)$.*

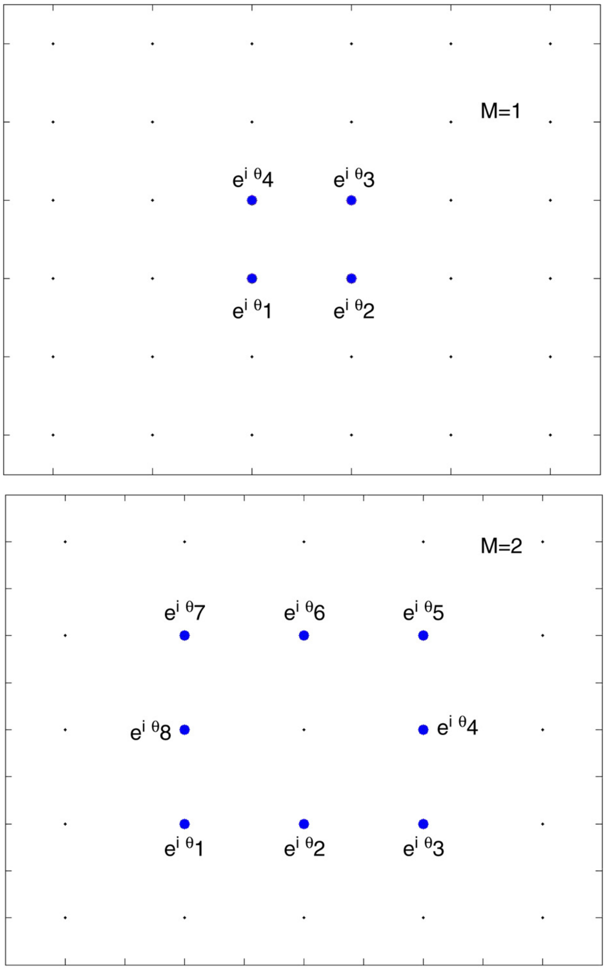

Fig. 1. Examples of the simple closed square contour S_M for $M = 1$ and $M = 2$.

Proof. Assume that $\phi_{n,m} \in \mathbb{R}$ for all $(n, m) \in \mathbb{Z}^2$. The difference equations (2.7) are rewritten as zeros of the nonlinear vector-valued function:

$$f_{n,m}(\boldsymbol{\phi}, \epsilon) = (1 - \phi_{n,m}^2)\phi_{n,m} - \epsilon \left(\phi_{n+1,m} + \phi_{n-1,m} + \phi_{n,m+1} + \phi_{n,m-1}\right) = 0. \tag{2.11}$$

The mapping $\mathbf{f} : \Omega \times \mathcal{O}(0) \mapsto \Omega$ is C^1 on $\boldsymbol{\phi} \in \Omega$ and has a bounded continuous Fréchet derivative, given by

$$\mathcal{L}_{n,m} = \left(1 - 3\phi_{n,m}^2\right) - \epsilon \left(s_{+1,0} + s_{-1,0} + s_{0,+1} + s_{0,-1}\right), \tag{2.12}$$

where $s_{n',m'}$ is the shift operator, such that $s_{n',m'} u_{n,m} = u_{n+n',m+m'}$. It is obvious that

$$\mathbf{f}(\boldsymbol{\phi}^{(0)}, 0) = \mathbf{0}, \qquad \ker(\mathcal{L}^{(0)}) = \emptyset, \tag{2.13}$$

where $\boldsymbol{\phi}^{(0)}$ is the discrete soliton for $\epsilon = 0$ (see Definition 2.1) and $\mathcal{L}^{(0)}$ is the operator $\mathcal{L}$ computed at $\boldsymbol{\phi} = \boldsymbol{\phi}^{(0)}$ and $\epsilon = 0$. It follows from (2.12) and (2.13) that $\mathcal{L}^{(0)} : \Omega \mapsto \Omega$ has a bounded inverse. By the Implicit Function Theorem [35, Appendix 1], there exists a local mapping $\boldsymbol{\phi} : \mathcal{O}(0) \to \Omega$, such that $\boldsymbol{\phi}(\epsilon)$ is at least continuous in

$\epsilon \in \mathcal{O}(0)$ and $\boldsymbol{\phi}^{(0)} = \boldsymbol{\phi}(0)$. Moreover, since $\mathbf{f}(\boldsymbol{\phi}, \epsilon)$ is analytic in $\epsilon \in \mathcal{O}(0)$, then $\boldsymbol{\phi}(\epsilon)$ is analytic in $\epsilon \in \mathcal{O}(0)$ [34, Chapter 2.2]. □

Remark 2.5. Proposition 2.4 does not exclude a possibility of continuation of the limiting solution (2.8) with $\theta_{n,m} = \{0, \pi\}$ for all $(n, m) \in S$ to the complex-valued solution $\boldsymbol{\phi}(\epsilon)$ in $\epsilon \in \mathcal{O}(0)$.

Proposition 2.6. *There exists a vector-valued function* $\mathbf{g} : \mathcal{T} \times \mathcal{O}(0) \mapsto \mathbb{R}^N$ *such that the limiting solution* (2.8) *is continued to the domain* $\epsilon \in \mathcal{O}(0)$ *if and only if* $\boldsymbol{\theta} \in \mathcal{T}$ *is a root of* $\mathbf{g}(\boldsymbol{\theta}, \epsilon) = \mathbf{0}$ *in* $\epsilon \in \mathcal{O}(0)$. *Moreover, the function* $\mathbf{g}(\boldsymbol{\theta}, \epsilon)$ *is analytic in* $\epsilon \in \mathcal{O}(0)$ *and* $\mathbf{g}(\boldsymbol{\theta}, 0) = \mathbf{0}$ *for any* $\boldsymbol{\theta} \in \mathcal{T}$.

Proof. When $\phi_{n,m} \in \mathbb{C}$ for some $(n, m) \in \mathbb{Z}^2$, the difference equations (2.7) are complemented by the complex conjugate equations in the abstract form:

$$\mathbf{f}(\boldsymbol{\phi}, \bar{\boldsymbol{\phi}}, \epsilon) = \mathbf{0}, \qquad \bar{\mathbf{f}}(\boldsymbol{\phi}, \bar{\boldsymbol{\phi}}, \epsilon) = \mathbf{0}. \tag{2.14}$$

Taking the Fréchet derivative of $\mathbf{f}(\boldsymbol{\phi}, \bar{\boldsymbol{\phi}}, \epsilon)$ with respect to $\boldsymbol{\phi}$ and $\bar{\boldsymbol{\phi}}$, we compute the linearization operator $\mathcal{H}$ for the difference equations (2.7):

$$\mathcal{H}_{n,m} = \begin{pmatrix} 1 - 2|\phi_{n,m}|^2 & -\phi_{n,m}^2 \\ -\bar{\phi}_{n,m}^2 & 1 - 2|\phi_{n,m}|^2 \end{pmatrix} - \epsilon(s_{+1,0} + s_{-1,0} + s_{0,+1} + s_{0,-1}) \begin{pmatrix} 1 & 0 \\ 0 & 1 \end{pmatrix}. \tag{2.15}$$

Let $\mathcal{H}^{(0)} = \mathcal{H}(\boldsymbol{\phi}^{(0)}, 0)$. It is clear that $\mathcal{H}^{(0)} : \Omega \times \Omega \mapsto \Omega \times \Omega$ is a self-adjoint Fredholm operator of index zero with $\dim \ker(\mathcal{H}^{(0)}) = N$. Moreover, eigenvectors of $\ker(\mathcal{H}^{(0)})$ renormalize the parameters $\theta_{n,m}$ for $(n, m) \in S$ in the limiting solution (2.8). By the Lyapunov Reduction Theorem [35, Chapter 7.1], there exists a decomposition $\Omega = \ker(\mathcal{H}^{(0)}) \oplus \omega$ such that $\mathbf{g}(\boldsymbol{\theta}, \epsilon)$ is defined in terms of the projections to $\ker(\mathcal{H}^{(0)})$. Let $\{\mathbf{e}_{n,m}\}_{(n,m)\in S}$ be a set of N linearly independent eigenvectors in the kernel of $\mathcal{H}^{(0)}$. It follows from the representation,

$$\mathcal{H}^{(0)}_{n,m} = -\begin{pmatrix} 1 & e^{2i\theta_{n,m}} \\ e^{-2i\theta_{n,m}} & 1 \end{pmatrix}, \qquad (n, m) \in S, \tag{2.16}$$

that each eigenvector $\mathbf{e}_{n,m}$ in the set $\{\mathbf{e}_{n,m}\}_{(n,m)\in S}$ has the only non-zero element $(e^{i\theta_{n,m}}, -e^{-i\theta_{n,m}})^{\mathrm{T}}$ at the (n, m)-th position of $(\mathbf{u}, \mathbf{w}) \in \Omega \times \Omega$. By projections of the nonlinear equations (2.14) to $\ker(\mathcal{H}^{(0)})$, we derive an implicit representation for the functions $\mathbf{g}(\boldsymbol{\theta}, \epsilon)$:

$$\begin{aligned}(n, m) \in S: \quad 2i g_{n,m}(\boldsymbol{\theta}, \epsilon) &= (1 - |\phi_{n,m}|^2)\left(e^{-i\theta_{n,m}}\phi_{n,m} - e^{i\theta_{n,m}}\bar{\phi}_{n,m}\right) \\ &\quad - \epsilon e^{-i\theta_{n,m}}\left(\phi_{n+1,m} + \phi_{n-1,m} + \phi_{n,m+1} + \phi_{n,m-1}\right) \\ &\quad + \epsilon e^{i\theta_{n,m}}\left(\bar{\phi}_{n+1,m} + \bar{\phi}_{n-1,m} + \bar{\phi}_{n,m+1} + \bar{\phi}_{n,m-1}\right),\end{aligned} \tag{2.17}$$

where the factor $(2i)$ is introduced for convenient notation. Let $\phi_{n,m} = e^{i\theta_{n,m}} u_{n,m}$ for $(n, m) \in S$ and $\phi_{n,m} = u_{n,m}$ for $(n, m) \in \mathbb{Z}^2 \setminus S$. Since eigenvectors of $\ker(\mathcal{H}^{(0)})$ are excluded from the solution $\boldsymbol{\phi}$ in $\omega \subset \Omega$, we have $u_{n,m} \in \mathbb{R}$ for $(n, m) \in S$ such that

$$\begin{aligned}(n, m) \in S: \quad -2i g_{n,m}(\boldsymbol{\theta}, \epsilon) &= \epsilon e^{-i\theta_{n,m}}\left(\phi_{n+1,m} + \phi_{n-1,m} + \phi_{n,m+1} + \phi_{n,m-1}\right) \\ &\quad - \epsilon e^{i\theta_{n,m}}\left(\bar{\phi}_{n+1,m} + \bar{\phi}_{n-1,m} + \bar{\phi}_{n,m+1} + \bar{\phi}_{n,m-1}\right)\end{aligned} \tag{2.18}$$

and $\mathbf{g}(\boldsymbol{\theta}, 0) = \mathbf{0}$ for any $\boldsymbol{\theta} \in \mathcal{T}$. Since $\mathbf{f}(\boldsymbol{\phi}, \bar{\boldsymbol{\phi}}, \epsilon)$ is analytic in $\epsilon \in \mathcal{O}(0)$, then $\mathbf{g}(\boldsymbol{\theta}, \epsilon)$ is analytic in $\epsilon \in \mathcal{O}(0)$ [35, Appendix 3]. □

Corollary 2.7. *The function* $\mathbf{g}(\boldsymbol{\theta}, \epsilon)$ *can be expanded into convergent Taylor series in* $\mathcal{O}(0)$*:*

$$\mathbf{g}(\boldsymbol{\theta}, \epsilon) = \sum_{k=1}^{\infty} \epsilon^k \mathbf{g}^{(k)}(\boldsymbol{\theta}), \qquad \mathbf{g}^{(k)}(\boldsymbol{\theta}) = \frac{1}{k!}\partial_\epsilon^k \mathbf{g}(\boldsymbol{\theta}, 0). \tag{2.19}$$

If the root $\boldsymbol{\theta}(\epsilon)$ of $\mathbf{g}(\boldsymbol{\theta},\epsilon)=\mathbf{0}$ is analytic in $\epsilon\in\mathcal{O}(0)$, then the solution $\boldsymbol{\phi}(\epsilon)$ is analytic in $\epsilon\in\mathcal{O}(0)$ such that

$$\boldsymbol{\phi}(\epsilon)=\boldsymbol{\phi}^{(0)}+\sum_{k=1}^{\infty}\epsilon^{k}\boldsymbol{\phi}^{(k)}, \tag{2.20}$$

where $\boldsymbol{\phi}^{(0)}$ is given by (2.8).

Lemma 2.8. *Let $\boldsymbol{\theta}(\epsilon)$ be a root of $\mathbf{g}(\boldsymbol{\theta},\epsilon)=\mathbf{0}$ in $\epsilon\in\mathcal{O}(0)$. An arbitrary shift $\boldsymbol{\theta}(\epsilon)+\theta_0\mathbf{p}_0$, where $\theta_0\in\mathbb{R}$ and $\mathbf{p}_0=(1,1,\ldots,1)^{\mathrm{T}}$, gives a one-parameter family of roots of $\mathbf{g}(\boldsymbol{\theta},\epsilon)=\mathbf{0}$ for the same ϵ.*

Proof. The statement follows from the symmetry of the difference equations (2.7) with respect to gauge transformation (2.4) (see [35, Chapter 7.3]). □

Proposition 2.9. *Let $\boldsymbol{\theta}_*$ be the root of $\mathbf{g}^{(1)}(\boldsymbol{\theta})=\mathbf{0}$ and $\mathcal{M}_1$ be the Jacobian matrix of $\mathbf{g}^{(1)}(\boldsymbol{\theta})$ at $\boldsymbol{\theta}=\boldsymbol{\theta}_*$. If the matrix $\mathcal{M}_1$ has a simple zero eigenvalue, there exists a unique (modulo gauge transformation) analytic continuation of the limiting solution (2.8) to the domain $\epsilon\in\mathcal{O}(0)$.*

Proof. By Lemma 2.8, the matrix $\mathcal{M}_1$ always has a non-empty kernel with the eigenvector $\mathbf{p}_0=(1,1,\ldots,1)$ due to gauge transformation. Let X_0 be the constrained subspace of $\mathbb{C}^N$:

$$X_0=\{\mathbf{u}\in\mathbb{C}^N:\ (\mathbf{p}_0,\mathbf{u})=0\}. \tag{2.21}$$

If the matrix $\mathcal{M}_1$ is non-singular in the subspace X_0, then there exists a unique (modulo the shift) analytic continuation of the root $\boldsymbol{\theta}_*$ in $\epsilon\in\mathcal{O}(0)$ by the Implicit Function Theorem, applied to the nonlinear equation $\mathbf{g}(\boldsymbol{\theta},\epsilon)=\mathbf{0}$ [35, Appendix 1]. □

Proposition 2.10. *Let $\boldsymbol{\theta}_*$ be a $(1+d)$-parameter solution of $\mathbf{g}^{(1)}(\boldsymbol{\theta})=\mathbf{0}$ and $\mathcal{M}_1$ have a zero eigenvalue of multiplicity $(1+d)$, where $1\le d\le N-1$. Let $\mathbf{g}^{(2)}(\boldsymbol{\theta}_*)=\cdots=\mathbf{g}^{(K-1)}(\boldsymbol{\theta}_*)=\mathbf{0}$ but $\mathbf{g}^{(K)}(\boldsymbol{\theta}_*)\neq\mathbf{0}$. The limiting solution (2.8) can be continued in the domain $\epsilon\in\mathcal{O}(0)$ only if $\mathbf{g}^{(K)}(\boldsymbol{\theta}_*)$ is orthogonal to* $\ker(\mathcal{M}_1)$.

Proof. Let $\mathbf{p}_0$ and $\{\mathbf{p}_l\}_{l=1}^{d}$ be eigenvectors of $\ker(\mathcal{M}_1)$. We define the constrained subspace of X_0:

$$X_d=\{\mathbf{u}\in X_0:\ (\mathbf{p}_l,\mathbf{u})=0,\ l=1,\ldots,d\}. \tag{2.22}$$

If $\mathbf{g}^{(K)}(\boldsymbol{\theta}_*)\notin X_d$, the Lyapunov–Schmidt Reduction Theorem in finite dimensions [35, Chapter 1.3] shows that the solution $\boldsymbol{\theta}_*$ cannot be continued in $\epsilon\in\mathcal{O}(0)$. □

Proposition 2.6 gives an abstract formulation of the continuation problem for the limiting solution (2.8) for $\epsilon\neq0$. Proposition 2.9 gives a sufficient condition for existence and uniqueness (up to gauge invariance) of such continuations. Proposition 2.10 gives a sufficient condition for termination of multi-parameter solutions. Particular applications of Propositions 2.6, 2.9 and 2.10 are limited by the complexity of the set S in the limiting solution (2.8), since computations of the vector-valued function $\mathbf{g}^{(1)}(\boldsymbol{\theta}),\mathbf{g}^{(2)}(\boldsymbol{\theta}),\ldots,\mathbf{g}^{(K)}(\boldsymbol{\theta})$ and the Jacobian matrix $\mathcal{M}_1$ could be technically involved. We apply the abstract results of Propositions 2.6, 2.9 and 2.10 to the square discrete contour S_M, defined in (2.9).

3. Persistence of discrete vortices

We consider discrete solitons and vortices on the contour S_M defined by (2.9). Let the set θ_j correspond to the ordered contour S_M, starting at $\theta_1=\theta_{1,1}$, $\theta_2=\theta_{2,1}$ and ending at $\theta_N=\theta_{1,2}$, where $N=4M$. In what follows, we use the periodic boundary conditions for θ_j on the circle from $j=1$ to $j=N$, such that $\theta_0=\theta_N$, $\theta_1=\theta_{N+1}$, and so on.

The discrete vortex has the charge L if the phase differences $\Delta\theta_j$ between two consecutive nodes add up to $2\pi L$ along the discrete contour S_M, where $\Delta\theta_j$ is defined within the fundamental branch $|\Delta\theta_j| \leq \pi$. By gauge transformation, we can always set $\theta_1 = 0$ for convenience. We will also choose $\theta_2 = \theta$ with $0 \leq \theta \leq \pi$ for convenience, which corresponds to discrete vortices with $L \geq 0$.

3.1. Solutions of the first-order reductions

Substituting the limiting solution $\phi^{(0)}_{n,m}$ in the bifurcation function (2.18), we find that $\mathbf{g}^{(1)}(\boldsymbol{\theta})$ in the Taylor series (2.19) is non-zero for the contour S_M and it takes the form

$$\mathbf{g}^{(1)}_j(\boldsymbol{\theta}) = \sin(\theta_j - \theta_{j+1}) + \sin(\theta_j - \theta_{j-1}), \qquad 1 \leq j \leq N. \tag{3.1}$$

The bifurcation equations $\mathbf{g}^{(1)}(\boldsymbol{\theta}) = \mathbf{0}$ are rewritten as a system of N nonlinear equations for N parameters $\theta_1, \theta_2, \ldots, \theta_N$ as follows:

$$\sin(\theta_2 - \theta_1) = \sin(\theta_3 - \theta_2) = \cdots = \sin(\theta_N - \theta_{N-1}) = \sin(\theta_1 - \theta_N). \tag{3.2}$$

We classify all solutions of the bifurcation equations (3.2) and give explicit examples for $M = 1$ and $M = 2$.

Proposition 3.1. *Let $a_j = \cos(\theta_{j+1} - \theta_j)$ for $1 \leq j \leq N$, such that $\theta_1 = 0$, $\theta_2 = \theta$, and $\theta_{N+1} = 2\pi L$, where $N = 4M$, $0 \leq \theta \leq \pi$ and L is the vortex charge. All solutions of the bifurcation equations (3.2) reduce to four families:*

(i) *Discrete solitons with $\theta = \{0, \pi\}$ and*

$$\theta_j = \{0, \pi\}, \qquad 3 \leq j \leq N, \tag{3.3}$$

such that the set $\{a_j\}_{j=1}^N$ includes l coefficients $a_j = 1$ and $N - l$ coefficients $a_j = -1$, where $0 \leq l \leq N$.

(ii) *Symmetric vortices of charge L with $\theta = \frac{\pi L}{2M}$, where $1 \leq L \leq 2M - 1$, and*

$$\theta_j = \frac{\pi L(j-1)}{2M}, \qquad 3 \leq j \leq N, \tag{3.4}$$

such that all N coefficients are the same: $a_j = a = \cos\left(\frac{\pi L}{2M}\right)$.

(iii) *One-parameter families of asymmetric vortices of charge $L = M$ with $0 < \theta < \pi$ and*

$$\theta_{j+1} - \theta_j = \begin{Bmatrix} \theta \\ \pi - \theta \end{Bmatrix} \bmod (2\pi), \qquad 2 \leq j \leq N, \tag{3.5}$$

such that the set $\{a_j\}_{j=1}^N$ includes $2M$ coefficients $a_j = \cos\theta$ and $2M$ coefficients $a_j = -\cos\theta$.

(iv) *Zero-parameter asymmetric vortices of charge $L \neq M$ and*

$$\theta = \theta_* = \frac{\pi}{2}\left(\frac{n + 2L - 4M}{n - 2M}\right), \qquad 1 \leq n \leq N - 1, \quad n \neq 2M, \tag{3.6}$$

such that the set $\{a_j\}_{j=1}^N$ includes n coefficients $a_j = \cos\theta_*$ and $N - n$ coefficients $a_j = -\cos\theta_*$ and the family (iv) *does not reduce to any of the families* (i)–(iii).

Proof. All solutions of the bifurcation equations (3.2) are given by the binary choice equations (3.5) in the two roots of the sine function on $\theta \in [0, 2\pi]$, where the first choice gives $a_j = \cos\theta$ and the second choice gives $a_j = -\cos\theta$. Let us assume that there are in total n first choices and $N - n$ second choices, where $1 \leq n \leq N$. Then, we have

$$\theta_{N+1} = n\theta + (N-n)(\pi - \theta) = (2n - N)\theta + (N-n)\pi = 2\pi L,$$

where L is the integer charge of the discrete vortex. There are only two solutions of the above equation. When θ is an arbitrary parameter, we have $n = \frac{N}{2} = 2M$ and $L = M$, which gives the one-parameter family (iii). When $\theta = \theta_*$ is fixed, we have

$$\theta_* = \frac{\pi}{2}\left(\frac{n + 2L - 4M}{n - 2M}\right).$$

When $n = N - 2L$, we have the family (i) with $N - 2L$ phases $\theta_j = 0$ and $2L$ phases $\theta_j = \pi$. Since the charge is not assigned to discrete solitons, parameter L could be half-integer: $L = (N - l)/2$, where $0 \leq l \leq N$. When $n = 4M$, we have the family (ii) for any $1 \leq L \leq 2M - 1$. Other choices of n, which are irreducible to the families (i)–(iii), produce the family (iv). □

Remark 3.2. The one-parameter family (iii) connects special solutions of the families (i) and (ii). When $\theta = 0$ and $\theta = \pi$, the family (iii) reduces to the family (i) with $l = 2M$. When $\theta = \frac{\pi}{2}$, the family (iii) reduces to the family (ii) with $L = M$. We shall call the corresponding solutions of family (i) the super-symmetric soliton and those of family (ii) the super-symmetric vortex.

Remark 3.3. There exist $N_1 = 2^{N-1}$ solutions of family (i), $N_2 = 2M - 1$ solutions of family (ii), and N_3 solutions of family (iii), where

$$N_3 = 2^{N-1} - \sum_{k=0}^{2M-1} \frac{N!}{k!(N-k)!}. \tag{3.7}$$

The number N_4 of solutions of family (iv) cannot be computed in general. We consider such solutions only in the explicit examples of $M = 1$ and $M = 2$.

Example ($M = 1$ ($N = 4$)). There are $N_1 = 8$ solutions of family (i), $N_2 = 1$ solution of family (ii), $N_3 = 3$ solutions of family (iii), and no solutions of family (iv). The only symmetric vortex is the vortex cell with $L = 1$ and $\theta = \frac{\pi}{2}$. The three one-parameter asymmetric vortices are given explicitly by

$$\text{(a) } \theta_1 = 0,\ \theta_2 = \theta,\ \theta_3 = \pi,\ \theta_4 = \pi + \theta \tag{3.8}$$

$$\text{(b) } \theta_1 = 0,\ \theta_2 = \theta,\ \theta_3 = 2\theta,\ \theta_4 = \pi + \theta \tag{3.9}$$

$$\text{(c) } \theta_1 = 0,\ \theta_2 = \theta,\ \theta_3 = \pi,\ \theta_4 = 2\pi - \theta. \tag{3.10}$$

Example ($M = 2$ ($N = 8$)). There are $N_1 = 128$ solutions of family (i), $N_2 = 3$ solutions of family (ii), $N_3 = 35$ solutions of family (iii), and $N_4 = 14$ solutions of family (iv). The three symmetric vortices have charge $L = 1$ ($\theta = \frac{\pi}{4}$), $L = 2$ ($\theta = \frac{\pi}{2}$), and $L = 3$ ($\theta = \frac{3\pi}{4}$). The one-parameter asymmetric vortices include 35 combinations of four upper choices and four lower choices in (3.5), starting with the following three solutions:

$$\text{(a) } \theta_1 = 0,\ \theta_2 = \theta,\ \theta_3 = 2\theta,\ \theta_4 = 3\theta,\ \theta_5 = 4\theta,\ \theta_6 = \pi + 3\theta,\ \theta_7 = 2\pi + 2\theta,\ \theta_8 = 3\pi + \theta,$$

$$\text{(b) } \theta_1 = 0,\ \theta_2 = \theta,\ \theta_3 = 2\theta,\ \theta_4 = 3\theta,\ \theta_5 = \pi + 2\theta,\ \theta_6 = \pi + 3\theta,\ \theta_7 = 2\pi + 2\theta,\ \theta_8 = 3\pi + \theta,$$

$$\text{(c) } \theta_1 = 0,\ \theta_2 = \theta,\ \theta_3 = 2\theta,\ \theta_4 = 3\theta,\ \theta_5 = \pi + 2\theta,\ \theta_6 = 2\pi + \theta,\ \theta_7 = 2\pi + 2\theta,\ \theta_8 = 3\pi + \theta,$$

and so on. The zero-parameter asymmetric vortices include seven combinations of vortices with $L = 1$ for seven phase differences $\frac{\pi}{6}$ and one phase difference $\frac{5\pi}{6}$ and seven combinations of vortices with $L = 3$ for one phase difference $\frac{\pi}{6}$ and seven phase differences $\frac{5\pi}{6}$.

3.2. Continuation of solutions of the first-order reductions

We compute the Jacobian matrix $\mathcal{M}_1$ from the bifurcation function $\mathbf{g}^{(1)}(\boldsymbol{\theta})$, given in (3.1):

$$(\mathcal{M}_1)_{i,j} = \begin{cases} \cos(\theta_{j+1}-\theta_j)+\cos(\theta_{j-1}-\theta_j), & i=j \\ -\cos(\theta_j-\theta_i), & i=j\pm 1 \\ 0, & |i-j|\geq 2 \end{cases} \tag{3.11}$$

subject to the periodic boundary conditions. The structure of the matrix $\mathcal{M}_1$ is defined by the coefficients $a_j = \cos(\theta_{j+1}-\theta_j)$ for $1 \leq j \leq N$. The same type of matrices occurs in the perturbation theory of continuous multi-pulse solitons in coupled NLS equations [36]. Three technical results establish the location of the eigenvalues of the matrix $\mathcal{M}_1$.

Lemma 3.4. *Let n_0, z_0, and p_0 be the numbers of negative, zero, and positive terms of $a_j = \cos(\theta_{j+1}-\theta_j)$, $1 \leq j \leq N$, such that $n_0+z_0+p_0 = N$. Let $n(\mathcal{M}_1)$, $z(\mathcal{M}_1)$, and $p(\mathcal{M}_1)$ be the numbers of negative, zero, and positive eigenvalues of the matrix $\mathcal{M}_1$, defined by (3.11). Assume that $z_0 = 0$ and write*

$$A_1 = \sum_{i=1}^{N}\prod_{j\neq i} a_j = \left(\prod_{i=1}^{N} a_i\right)\left(\sum_{i=1}^{N}\frac{1}{a_i}\right). \tag{3.12}$$

If $A_1 \neq 0$, then $z(\mathcal{M}_1) = 1$, and either $n(\mathcal{M}_1) = n_0-1$, $p(\mathcal{M}_1) = p_0$ or $n(\mathcal{M}_1) = n_0$, $p(\mathcal{M}_1) = p_0-1$. Moreover, $n(\mathcal{M}_1)$ is even if $A_1 > 0$ and is odd if $A_1 < 0$. If $A_1 = 0$, then $z(\mathcal{M}_1) \geq 2$.

Proof. The first statement follows from [36, Appendix A]. Let the determinant equation be $D(\lambda) = \det(\mathcal{M}_1 - \lambda I) = 0$. By induction arguments in [36,37], it can be found that $D(0) = 0$ and $D'(0) = -NA_1$. On the other hand, $D'(0) = -\lambda_1\lambda_2\cdots\lambda_{N-1}$, where $\lambda_N = 0$ (which exists always with the eigenvector $\mathbf{p}_0 = (1,1,\ldots,1)^{\mathrm{T}}$; see Proposition 2.9). Then, it is clear that $(-1)^{n(\mathcal{M}_1)} = \mathrm{sign}(A_1)$. When $A_1 = 0$, at least one more eigenvalue is zero, such that $z(\mathcal{M}_1) \geq 2$. □

Lemma 3.5. *Let all coefficients $a_j = \cos(\theta_{j+1}-\theta_j)$, $1 \leq j \leq N$, be the same: $a_j = a$. Eigenvalues of the matrix $\mathcal{M}_1$ are computed explicitly as follows:*

$$\lambda_n = 4a\sin^2\frac{\pi n}{N}, \qquad 1 \leq n \leq N. \tag{3.13}$$

Proof. When $a_j = a$, $1 \leq j \leq N$, the eigenvalue problem for the matrix $\mathcal{M}_1$ takes the form of the linear difference equations with constant coefficients:

$$a\left(2x_j - x_{j+1} - x_{j-1}\right) = \lambda x_j, \qquad x_0 = x_N,\ x_1 = x_{N+1}, \tag{3.14}$$

The discrete Fourier mode $x_j = \exp\left(\mathrm{i}\frac{2\pi jn}{N}\right)$ for $1 \leq j, n \leq N$ results in the solution (3.13). □

Lemma 3.6. *Let all coefficients $a_j = \cos(\theta_{j+1}-\theta_j)$, $1 \leq j \leq N$, alternate the sign as $a_j = (-1)^j a$, where $N = 4M$. Eigenvalues of the matrix $\mathcal{M}_1$ are computed explicitly as follows:*

$$\lambda_n = -\lambda_{n+2M} = 2a\sin\frac{\pi n}{2M}, \qquad 1 \leq n \leq 2M, \tag{3.15}$$

such that $n(\mathcal{M}_1) = 2M-1$, $z(\mathcal{M}_1) = 2$, and $p(\mathcal{M}_1) = 2M-1$. These numbers do not change if the set $\{a_j\}_{j=1}^{N}$ is obtained from the sign-alternating set $\{(-1)^j a\}_{j=1}^{N}$ by permutations.

Proof. When $a_j = (-1)^j a$, $1 \leq j \leq 4M$, the eigenvalue problem for the matrix $\mathcal{M}_1$ takes the form of a coupled system of linear difference equations with constant coefficients:

$$a\left(y_j - y_{j-1}\right) = \lambda x_j, \qquad a\left(x_j - x_{j+1}\right) = \lambda y_j, \qquad 1 \leq j \leq 2M, \tag{3.16}$$

subject to the periodic boundary conditions: $x_1 = x_{2M+1}$ and $y_0 = y_{2M}$. The discrete Fourier mode $x_j =$

$x_0 \exp\left(i\frac{2\pi jn}{2M}\right)$ and $y_j = y_0 \exp\left(i\frac{2\pi jn}{2M}\right)$ for $1 \le j, n \le 2M$ results in the solution (3.15). In this case, we have $n(\mathcal{M}_1) = 2M - 1$, $z(\mathcal{M}_1) = 2$, and $p(\mathcal{M}_1) = 2M - 1$, such that $D(0) = D'(0) = 0$ and $D''(0) < 0$ in the determinant equation $D(\lambda) = \det(\mathcal{M}_1 - \lambda I)$. In order to prove that $z(\mathcal{M}_1) = 2$ remains invariant with respect to permutations of the sign-alternating set $\{(-1)^j a\}_{j=1}^N$, we find with the aid of Mathematica that

$$D''(0) = \left(\prod_{i=1}^N a_i\right)\left(\alpha_N\left(\sum_{i=1}^{N-1}\frac{1}{a_i a_{i+1}} + \frac{1}{a_1 a_N}\right) + \beta_N\left(\sum_{i=1}^{N-2}\sum_{l=i+2}^{N}\frac{1}{a_i a_l} - \frac{1}{a_1 a_N}\right)\right), \tag{3.17}$$

where $0 < \alpha_N < \beta_N$ are numerical coefficients. Let A_* denote the sign-alternating set $\{(-1)^j a\}_{j=1}^N$ and A denote a set obtained from A_* by permutations. It is clear that

$$\left(\sum_{i=1}^{N-1}\frac{1}{a_i a_{i+1}} + \frac{1}{a_1 a_N}\right)_{A_*} \le \left(\sum_{i=1}^{N-1}\frac{1}{a_i a_{i+1}} + \frac{1}{a_1 a_N}\right)_{A}$$

and

$$\left(\sum_{i=1}^{N-1}\sum_{l=i+1}^{N}\frac{1}{a_i a_l}\right)_{A_*} = \left(\sum_{i=1}^{N-1}\sum_{l=i+1}^{N}\frac{1}{a_i a_l}\right)_{A}.$$

Therefore, the expression in brackets in (3.17) can be estimated as follows:

$$\begin{aligned}
&(\alpha_N - \beta_N)\left(\sum_{i=1}^{N-1}\frac{1}{a_i a_{i+1}} + \frac{1}{a_1 a_N}\right)_{A} + \beta_N\left(\sum_{i=1}^{N-1}\sum_{l=i+1}^{N}\frac{1}{a_i a_l}\right)_{A} \\
&\quad \le (\alpha_N - \beta_N)\left(\sum_{i=1}^{N-1}\frac{1}{a_i a_{i+1}} + \frac{1}{a_1 a_N}\right)_{A_*} + \beta_N\left(\sum_{i=1}^{N-1}\sum_{l=i+1}^{N}\frac{1}{a_i a_l}\right)_{A_*} < 0,
\end{aligned}$$

where the last inequality follows from the fact that $D''(0) < 0$ for A_*. Therefore, $z(\mathcal{M}_1) = 2$ for the set A. Combining it with estimates from [36, Appendix A], we have $n(\mathcal{M}_1) = p(\mathcal{M}_1) = 2M - 1$ for the set A. □

Using Lemmas 3.4–3.6, we classify continuations of solutions of the first-order reductions (see families (i)–(iv) of Proposition 3.1).

For family (i), excluding the case of super-symmetric solitons (see Remark 3.2), the numbers of positive and negative signs of a_j are different, such that the conditions $z_0 = 0$ and $A_1 \neq 0$ are satisfied in Lemma 3.4, and hence $z(\mathcal{M}_1) = 1$. By Proposition 2.9, the family (i) has a unique continuation to discrete solitons (see Definition 2.1). This result agrees with Proposition 2.4. Continuations described in Remark 2.5 are only possible for super-symmetric solitons.

For family (ii), all coefficients a_j are the same: $a_j = a = \cos\left(\frac{\pi L}{2M}\right)$, $1 \le j \le N$. By Lemma 3.5, there is always a zero eigenvalue ($\lambda_N = 0$), while the remaining $(N - 1)$ eigenvalues are all positive for $a > 0$ (when $1 \le L \le M - 1$), negative for $a < 0$ (when $M + 1 \le L \le 2M - 1$), and zero for $a = 0$ (when $L = M$). By Proposition 2.9, the family (ii), excluding the case of super-symmetric vortices (see Remark 3.2), has a unique continuation to symmetric vortices with charge L, where $1 \le L \le 2M - 1$ and $L \neq M$ (see Definitions 2.2 and 2.3).

For family (iii), there are $2M$ coefficients $a_j = \cos\theta$ and $2M$ coefficients $a_j = -\cos\theta$, which are non-zero for $\theta \neq \frac{\pi}{2}$. By Lemma 3.6, we have $n(\mathcal{M}_1) = 2M - 1$, $z(\mathcal{M}_1) = 2$, and $p(\mathcal{M}_1) = 2M - 1$. The additional zero eigenvalue is related to the derivative of the family of the asymmetric discrete vortices (3.5) with respect to the parameter θ. Therefore, continuations of family (iii) of asymmetric vortices, including the particular cases of super-symmetric solitons of family (i) and super-symmetric vortices of family (ii), must be considered beyond the first-order reductions.

For family (iv), since $n \neq 2M$, the conditions $z_0 = 0$ and $A_1 \neq 0$ are satisfied in Lemma 3.4, and hence $z(\mathcal{M}_1) = 1$. By Proposition 2.9, the family (iv) has a unique continuation to asymmetric vortices for $\epsilon \neq 0$.

3.3. Continuation of solutions to the second-order reductions

Results of the first-order reductions are insufficient for concluding persistence of the asymmetric vortices of family (iii), including the super-symmetric soliton of family (i) and the super-symmetric vortex of family (ii). Therefore, we continue the bifurcation function $\mathbf{g}(\boldsymbol{\theta}, \epsilon)$ to the second order of ϵ in the Taylor series (2.19). It follows from (2.7) that the first-order correction of the Taylor series (2.20) satisfies the inhomogeneous problem:

$$(1 - 2|\phi_{n,m}^{(0)}|^2)\phi_{n,m}^{(1)} - \phi_{n,m}^{(0)2}\bar{\phi}_{n,m}^{(1)} = \phi_{n+1,m}^{(0)} + \phi_{n-1,m}^{(0)} + \phi_{n,m+1}^{(0)} + \phi_{n,m-1}^{(0)}. \tag{3.18}$$

We define the solution of the inhomogeneous problem (3.18) in $\omega \subset \Omega$, so that the homogeneous solutions in $\ker(\mathcal{H}^{(0)})$ are removed from the solution $\boldsymbol{\phi}^{(1)}$. This is equivalent to the constraint: $\phi_{n,m} = u_{n,m} e^{i\theta_{n,m}}$, $u_{n,m} \in \mathbb{R}$, for all $(n, m) \in S_M$. We develop computations for three distinct cases: $M = 1$, $M = 2$ and $M \geq 3$. This separation is due to the special structure of the discrete contours S_M.

Case $M = 1$: The inhomogeneous problem (3.18) has a unique solution $\boldsymbol{\phi}^{(1)} \in \omega \subset \Omega$:

$$\phi_{n,m}^{(1)} = -\frac{1}{2}\left[\cos(\theta_{j-1} - \theta_j) + \cos(\theta_{j+1} - \theta_j)\right] e^{i\theta_j}, \tag{3.19}$$

where the index j enumerates the node (n, m) on the contour S_M,

$$\phi_{n,m}^{(1)} = e^{i\theta_j}, \tag{3.20}$$

where the node (n, m) is adjacent to the j-th node on the contour S_M, while $\phi_{n,m}^{(1)}$ is zero for all remaining nodes. By substituting the first-order correction term $\phi_{n,m}^{(1)}$ into the bifurcation function (2.18), we find the correction term $\mathbf{g}^{(2)}(\boldsymbol{\theta})$ in the Taylor series (2.19):

$$\begin{aligned}\mathbf{g}_j^{(2)}(\boldsymbol{\theta}) = {} & \frac{1}{2}\sin(\theta_{j+1} - \theta_j)\left[\cos(\theta_j - \theta_{j+1}) + \cos(\theta_{j+2} - \theta_{j+1})\right] \\ & + \frac{1}{2}\sin(\theta_{j-1} - \theta_j)\left[\cos(\theta_j - \theta_{j-1}) + \cos(\theta_{j-2} - \theta_{j-1})\right], \qquad 1 \leq j \leq N.\end{aligned} \tag{3.21}$$

We compute the vector $\mathbf{g}_2 = \mathbf{g}^{(2)}(\boldsymbol{\theta})$ at the asymmetric vortex solutions (3.8)–(3.10):

$$\text{(a) } \mathbf{g}_2 = \begin{pmatrix} 0 \\ 0 \\ 0 \\ 0 \end{pmatrix}, \qquad \text{(b) } \mathbf{g}_2 = \begin{pmatrix} 2 \\ 0 \\ -2 \\ 0 \end{pmatrix} \sin\theta\cos\theta, \qquad \text{(c) } \mathbf{g}_2 = \begin{pmatrix} 0 \\ -2 \\ 0 \\ 2 \end{pmatrix} \sin\theta\cos\theta.$$

The kernel of $\mathcal{M}_1$ is two-dimensional with the eigenvectors $\mathbf{p}_0 = (1, 1, 1, 1)^{\mathrm{T}}$ and $\mathbf{p}_1$. The eigenvector $\mathbf{p}_1$ is related to derivatives of the solutions (3.8)–(3.10) in θ:

$$\text{(a) } \mathbf{p}_1 = \begin{pmatrix} 0 \\ 1 \\ 0 \\ 1 \end{pmatrix}, \qquad \text{(b) } \mathbf{p}_1 = \begin{pmatrix} 0 \\ 1 \\ 2 \\ 1 \end{pmatrix}, \qquad \text{(c) } \mathbf{p}_1 = \begin{pmatrix} 0 \\ 1 \\ 0 \\ -1 \end{pmatrix}.$$

The Fredholm alternative $(\mathbf{p}_1, \mathbf{g}_2) = 0$ is satisfied for the solution (a) but fails for the solutions (b) and (c), unless $\theta = \{0, \frac{\pi}{2}, \pi\}$. The latter cases are included in the definitions of super-symmetric discrete solitons and vortices (see Remark 3.2). By Proposition 2.10 with $K = 2$, the solutions (b) and (c) cannot be continued in $\epsilon \neq 0$, while the solution (a) can be continued up to the second-order reductions.

Case $M = 2$: The solution $\boldsymbol{\phi}^{(1)} \in \omega \subset \Omega$ of the inhomogeneous problem (3.18) is given by (3.19) and (3.20), except for the center node (2, 2), where

$$\phi_{2,2}^{(1)} = \mathrm{e}^{\mathrm{i}\theta_2} + \mathrm{e}^{\mathrm{i}\theta_4} + \mathrm{e}^{\mathrm{i}\theta_6} + \mathrm{e}^{\mathrm{i}\theta_8}. \tag{3.22}$$

The correction term $\mathbf{g}^{(2)}(\boldsymbol{\theta})$ is given by (3.21) but the even entries are modified as follows:

$$\mathbf{g}_j^{(2)}(\boldsymbol{\theta}) \to \mathbf{g}_j^{(2)}(\boldsymbol{\theta}) + \sin(\theta_j - \theta_{j-2}) + \sin(\theta_j - \theta_{j+2}) + \sin(\theta_j - \theta_{j+4}), \qquad j = 2, 4, 6, 8. \tag{3.23}$$

The vector $\mathbf{g}_2 = \mathbf{g}^{(2)}(\boldsymbol{\theta})$ can be computed for each of 35 one-parameter asymmetric vortex solutions, starting with the first three solutions:

$$\text{(a) } \mathbf{g}_2 = \begin{pmatrix} 2 \\ 1 \\ 0 \\ -1 \\ -2 \\ -1 \\ 0 \\ 1 \end{pmatrix} \sin\theta\cos\theta, \quad \text{(b) } \mathbf{g}_2 = \begin{pmatrix} 2 \\ 1 \\ -1 \\ -1 \\ 0 \\ -1 \\ -1 \\ 1 \end{pmatrix} \sin\theta\cos\theta, \quad \text{(c) } \mathbf{g}_2 = \begin{pmatrix} 2 \\ 1 \\ -1 \\ -2 \\ 0 \\ 1 \\ -1 \\ 0 \end{pmatrix} \sin\theta\cos\theta.$$

The second eigenvector $\mathbf{p}_1$ of the kernel of $\mathcal{M}_1$ is related to derivatives of the family in θ, e.g.

$$\text{(a) } \mathbf{p}_1 = \begin{pmatrix} 0 \\ 1 \\ 2 \\ 3 \\ 4 \\ 3 \\ 2 \\ 1 \end{pmatrix}, \quad \text{(b) } \mathbf{p}_1 = \begin{pmatrix} 0 \\ 1 \\ 2 \\ 3 \\ 2 \\ 3 \\ 2 \\ 1 \end{pmatrix}, \quad \text{(c) } \mathbf{p}_1 = \begin{pmatrix} 0 \\ 1 \\ 2 \\ 3 \\ 2 \\ 1 \\ 2 \\ 1 \end{pmatrix}.$$

Assuming that $\theta \neq \{0, \frac{\pi}{2}, \pi\}$, the Fredholm alternative condition $(\mathbf{p}_1, \mathbf{g}_2) = 0$ fails for all solutions of family (iii) but one. The only solution of family (iii), where $\mathbf{g}_2 = \mathbf{0}$, is characterized by the alternating signs of coefficients $a_j = \cos(\theta_{j+1} - \theta_j)$ for $1 \leq j \leq N$.

Case $M \geq 3$: The solution $\boldsymbol{\phi}^{(1)} \in \omega \subset \Omega$ of the inhomogeneous problem (3.18) is given by (3.19) and (3.20), except for the four interior corner nodes $(2, 2)$,$(M, 2)$,(M, M), and $(2, M)$, where

$$\phi_{n,m}^{(1)} = \mathrm{e}^{\mathrm{i}\theta_{j-1}} + \mathrm{e}^{\mathrm{i}\theta_{j+1}}, \qquad j = 1, M+1, 2M+1, 3M+1. \tag{3.24}$$

The correction term $\mathbf{g}^{(2)}(\boldsymbol{\theta})$ is given by (3.21), except for the adjacent entries to the four corner nodes on the contour S_M: $(1, 1)$, $(1, M+1)$, $(M+1, M+1)$, and $(M+1, 1)$, which are modified by

$$\begin{aligned} \mathbf{g}_j^{(2)}(\boldsymbol{\theta}) &\to \mathbf{g}_j^{(2)}(\boldsymbol{\theta}) + \sin(\theta_j - \theta_{j-2}), \qquad j = 2, M+2, 2M+2, 3M+2, \\ \mathbf{g}_j^{(2)}(\boldsymbol{\theta}) &\to \mathbf{g}_j^{(2)}(\boldsymbol{\theta}) + \sin(\theta_j - \theta_{j+2}), \qquad j = M, 2M, 3M, 4M. \end{aligned} \tag{3.25}$$

For any $M \geq 3$, there is a solution of family (iii), where $\mathbf{g}_2 = \mathbf{0}$, which is characterized by the alternating signs of coefficients $a_j = \cos(\theta_{j+1} - \theta_j)$ for $1 \leq j \leq N$. In the case $M = 3$, we have checked that all other solutions of family (iii) have $(\mathbf{p}_1, \mathbf{g}_2) \neq 0$ and hence terminate at the second-order reductions.

By Proposition 2.10 with $K = 2$, all asymmetric vortices of family (iii), except for the sign-alternating set $a_j = \cos(\theta_{j+1} - \theta_j) = (-1)^{j+1}\cos\theta$, $1 \leq j \leq N$, cannot be continued to $\epsilon \neq 0$ for $M = 1, 2, 3$. The only solution which can be continued up to the second-order reductions has the explicit form

$$\theta_{4j-3} = 2\pi(j-1), \quad \theta_{4j-2} = \theta_{4j-3} + \theta, \qquad \theta_{4j-1} = \theta_{4j-3} + \pi, \quad \theta_{4j} = \theta_{4j-3} + \pi + \theta, \tag{3.26}$$

where $1 \leq j \leq M$ and $0 \leq \theta \leq \pi$. This solution includes two particular cases of super-symmetric solitons of family (i) for $\theta = 0$ and $\theta = \pi$ and super-symmetric vortices of family (ii) for $\theta = \frac{\pi}{2}$. Continuation of the solution (3.26) must be considered beyond the second-order reductions.

Based on these computations, we also consider continuations of super-symmetric solitons of family (i). Let $\mathcal{M}_2$ be the Jacobian matrix computed from the bifurcation function $\mathbf{g}^{(2)}(\boldsymbol{\theta})$, given in (3.21), (3.23) and (3.25). Since $(\mathbf{p}_1, \mathbf{g}_2) \neq 0$ for $\theta \neq \{0, \frac{\pi}{2}, \pi\}$, except for the case of the sign-alternating set $\{(-1)^j a\}_{j=1}^N$, it follows from regular perturbation theory that $(\mathbf{p}_1, \mathcal{M}_2\mathbf{p}_1) \neq 0$. Therefore, the second zero eigenvalue of $\mathcal{M}_1$ bifurcates off zero for the matrix $\mathcal{M}_1 + \epsilon\mathcal{M}_2$. By Proposition 2.9 (which needs to be modified for the Jacobian matrix $\mathcal{M}_1 + \epsilon\mathcal{M}_2$), the super-symmetric solutions of family (i), which are different from the sign-alternating set $\{(-1)^j a\}_{j=1}^N$, are uniquely continued to discrete solitons (see Definition 2.1). Continuations described in Remark 2.5 are only possible for super-symmetric solitons with the sign-alternating set $\{(-1)^j a\}_{j=1}^N$.

3.4. Jacobian matrix of the second-order reductions

The Jacobian matrix $\mathcal{M}_1$ of the first-order reductions is zero identically for super-symmetric vortices of family (ii) with $L = M$. In order to study stability of super-symmetric vortices, we will need to the Jacobian matrix $\mathcal{M}_2$, which is computed from the second-order bifurcation function $\mathbf{g}^{(2)}(\boldsymbol{\theta})$, given in (3.21), (3.23) and (3.25). These computations are developed separately for three cases $M = 1$, $M = 2$, and $M \geq 3$.

Case $M = 1$: Non-zero elements of $\mathcal{M}_2$ are given by

$$(\mathcal{M}_2)_{i,j} = \begin{cases} +1, & i = j \\ -\dfrac{1}{2}, & i = j \pm 2 \\ 0, & |i-j| \neq 0, 2 \end{cases} \tag{3.27}$$

or explicitly

$$\mathcal{M}_2 = \begin{pmatrix} 1 & 0 & -1 & 0 \\ 0 & 1 & 0 & -1 \\ -1 & 0 & 1 & 0 \\ 0 & -1 & 0 & 1 \end{pmatrix}. \tag{3.28}$$

The matrix $\mathcal{M}_2$ has four eigenvalues: $\lambda_1 = \lambda_2 = 2$ and $\lambda_3 = \lambda_4 = 0$. The two eigenvectors for the zero eigenvalue are $\mathbf{p}_3 = (1, 0, 1, 0)^{\mathrm{T}}$ and $\mathbf{p}_4 = (0, 1, 0, 1)^{\mathrm{T}}$. The eigenvector $\mathbf{p}_4$ corresponds to the derivative of the asymmetric vortex (3.8) with respect to parameter θ, while the eigenvector $\mathbf{p}_0 = \mathbf{p}_3 + \mathbf{p}_4$ corresponds to the shift due to gauge transformation.

Case $M = 2$: The Jacobian matrix $\mathcal{M}_2$ is given in (3.27) except for the even entries. The modified Jacobian matrix $\tilde{\mathcal{M}}_2$ has the form

$$\tilde{\mathcal{M}}_2 = \mathcal{M}_2 + \Delta\mathcal{M}_2, \tag{3.29}$$

where $\Delta\mathcal{M}_2$ is a rank-one non-positive matrix with the elements

$$(\Delta\mathcal{M}_2)_{i,j} = \begin{cases} -1, & i = j \\ +1, & i = j \pm 2 \qquad j = 2, 4, 6, 8 \\ -1, & i = j \pm 4 \end{cases} \tag{3.30}$$

and all other elements are zeros. The explicit form for the modified matrix $\tilde{\mathcal{M}}_2$ is

$$\tilde{\mathcal{M}}_2 = \begin{pmatrix} 1 & 0 & -\frac{1}{2} & 0 & 0 & 0 & -\frac{1}{2} & 0 \\ 0 & 0 & 0 & \frac{1}{2} & 0 & -1 & 0 & \frac{1}{2} \\ -\frac{1}{2} & 0 & 1 & 0 & -\frac{1}{2} & 0 & 0 & 0 \\ 0 & \frac{1}{2} & 0 & 0 & 0 & \frac{1}{2} & 0 & -1 \\ 0 & 0 & -\frac{1}{2} & 0 & 1 & 0 & -\frac{1}{2} & 0 \\ 0 & -1 & 0 & \frac{1}{2} & 0 & 0 & 0 & \frac{1}{2} \\ -\frac{1}{2} & 0 & 0 & 0 & -\frac{1}{2} & 0 & 1 & 0 \\ 0 & \frac{1}{2} & 0 & -1 & 0 & \frac{1}{2} & 0 & 0 \end{pmatrix}. \tag{3.31}$$

The eigenvalue problem for $\tilde{\mathcal{M}}_2$ decouples into two linear difference equations with constant coefficients:

$$2x_j - x_{j+1} - x_{j-1} = 2\lambda x_j, \qquad j = 1, 2, 3, 4$$
$$-2y_{j+2} + y_{j+1} + y_{j-1} = 2\lambda y_j, \qquad j = 1, 2, 3, 4,$$

subject to the periodic boundary conditions for x_j and y_j. By the discrete Fourier transform (see the proof of Lemma 3.6), the first problem has eigenvalues $\lambda_1 = 1$, $\lambda_2 = 2$, $\lambda_3 = 1$, and $\lambda_4 = 0$, while the second problem has eigenvalues $\lambda_5 = 1$, $\lambda_6 = -2$, $\lambda_7 = 1$, and $\lambda_8 = 0$. The two eigenvectors for the zero eigenvalue are $\mathbf{p}_4 = (1, 0, 1, 0, 1, 0, 1, 0)^{\mathrm{T}}$ and $\mathbf{p}_8 = (0, 1, 0, 1, 0, 1, 0, 1)^{\mathrm{T}}$, where the eigenvector $\mathbf{p}_8$ corresponds to the derivative of the asymmetric vortex (3.26) with respect to parameter θ and the eigenvector $\mathbf{p}_0 = \mathbf{p}_4 + \mathbf{p}_8$ corresponds to the shift due to gauge transformation.

Case $M \geq 3$: The Jacobian matrix $\mathcal{M}_2$ is given in (3.27), except for the adjacent entries to the four corner nodes on the contours S_M: $(1, 1)$, $(1, M + 1)$, $(M + 1, M + 1)$, and $(M + 1, 1)$. The modified Jacobian matrix $\tilde{\mathcal{M}}_2$ has the form

$$\tilde{\mathcal{M}}_2 = \mathcal{M}_2 + \Delta\mathcal{M}_2, \tag{3.32}$$

where $\Delta\mathcal{M}_2$ is a rank-four non-positive matrix with the elements

$$(\Delta\mathcal{M}_2)_{i,j} = \begin{cases} -1, & i = j = 2, M, M + 2, 2M, 2M + 2, 3M, 3M + 2, 4M \\ +1, & i = j - 2 = M, 2M, 3M, 4M \\ +1, & i = j + 2 = 2, M + 2, 2M + 2, 3M + 2 \end{cases} \tag{3.33}$$

and all other elements are zeros. The explicit form for the modified matrix $\tilde{\mathcal{M}}_2$ in the case $M = 3$ is

$$\tilde{\mathcal{M}}_2 = \begin{pmatrix} 1 & 0 & -\frac{1}{2} & 0 & 0 & 0 & 0 & 0 & 0 & 0 & -\frac{1}{2} & 0 \\ 0 & 0 & 0 & -\frac{1}{2} & 0 & 0 & 0 & 0 & 0 & 0 & 0 & \frac{1}{2} \\ -\frac{1}{2} & 0 & 0 & 0 & \frac{1}{2} & 0 & 0 & 0 & 0 & 0 & 0 & 0 \\ 0 & -\frac{1}{2} & 0 & 1 & 0 & -\frac{1}{2} & 0 & 0 & 0 & 0 & 0 & 0 \\ 0 & 0 & \frac{1}{2} & 0 & 0 & 0 & -\frac{1}{2} & 0 & 0 & 0 & 0 & 0 \\ 0 & 0 & 0 & -\frac{1}{2} & 0 & 0 & 0 & \frac{1}{2} & 0 & 0 & 0 & 0 \\ 0 & 0 & 0 & 0 & -\frac{1}{2} & 0 & 1 & 0 & -\frac{1}{2} & 0 & 0 & 0 \\ 0 & 0 & 0 & 0 & 0 & \frac{1}{2} & 0 & 0 & 0 & -\frac{1}{2} & 0 & 0 \\ 0 & 0 & 0 & 0 & 0 & 0 & -\frac{1}{2} & 0 & 0 & 0 & \frac{1}{2} & 0 \\ 0 & 0 & 0 & 0 & 0 & 0 & 0 & -\frac{1}{2} & 0 & 1 & 0 & -\frac{1}{2} \\ -\frac{1}{2} & 0 & 0 & 0 & 0 & 0 & 0 & 0 & \frac{1}{2} & 0 & 0 & 0 \\ 0 & \frac{1}{2} & 0 & 0 & 0 & 0 & 0 & 0 & 0 & -\frac{1}{2} & 0 & 0 \end{pmatrix}. \tag{3.34}$$

The eigenvalue problem for $\tilde{\mathcal{M}}_2$ decouples into eigenvalue problems for two 6-by-6 matrices, which are related by the Toeplitz transformation. As a result, the spectra of these two matrices are identical with the eigenvalues, obtained with the use of MATLAB:

$$\lambda_1 = \lambda_7 = -0.780776, \quad \lambda_2 = \lambda_8 = -0.5, \quad \lambda_3 = \lambda_9 = 0,$$
$$\lambda_4 = \lambda_{10} = 0.5, \quad \lambda_5 = \lambda_{11} = 1.28078, \quad \lambda_6 = \lambda_{12} = 1.5.$$

The matrix $\tilde{\mathcal{M}}_2$ has exactly two zero eigenvalues, one of which is related to the derivative of the asymmetric vortex (3.26) in θ and the other one to the shift due to gauge transformation.

Computations of the matrix $\mathcal{M}_2$ for super-symmetric vortices of family (ii) in the cases $M = 1, 2, 3$ confirm the results of the second-order reductions for asymmetric vortices of family (iii) in those cases. Although all N_3 solutions of family (iii) reduce to the super-symmetric vortex of family (ii) in the first-order reductions, it is the only family (3.26) that survives in the second-order reductions, such that the super-symmetric vortex of family (ii) with $L = M$ and $\theta = \frac{\pi}{2}$ can be deformed along an appropriate eigenvector $\mathbf{p}_1$ and continued up to the second-order reductions to the asymmetric vortex (3.26).

3.5. Higher-order reductions

The presence of the arbitrary parameter θ in the family of asymmetric vortices (3.26) is not supported by the symmetry of the discrete contour S_M or by the symmetry of the discrete NLS lattice (2.1). According to Proposition 2.10, we would expect therefore that the one-parameter family (3.26) do not persist beyond all orders of the Lyapunov–Schmidt reductions. This would imply that zeros of $\mathbf{g}^{(1)}(\boldsymbol{\theta})$ are destroyed in a higher-order term $\mathbf{g}^{(K)}(\boldsymbol{\theta})$ of the Taylor series (2.19) for $\mathbf{g}(\boldsymbol{\theta}, \epsilon)$. In order to confirm this conjecture, we develop a MATLAB-assisted algorithm.

Let M be the index of the discrete contour S_M and K be the truncation order of the Lyapunov–Schmidt reduction. We construct a square domain $(n, m) \in D(M, K)$ which includes N_0-by-N_0 lattice nodes, where $N_0 = 2K+M+1$.

Corrections of the power series (2.20) for a given configuration of $\boldsymbol{\theta}$ in (3.26) solve the set of inhomogeneous equations

$$\mathcal{H}^{(0)} \begin{pmatrix} \boldsymbol{\phi}^{(k)} \\ \bar{\boldsymbol{\phi}}^{(k)} \end{pmatrix} = \begin{pmatrix} \mathbf{f}^{(k)} \\ \bar{\mathbf{f}}^{(k)} \end{pmatrix}, \qquad 1 \le k \le K,$$

where $\mathcal{H}^{(0)}$ is given by (2.16) and $\mathbf{f}^{(k)}$ is the right-hand-side terms, which are defined recursively from the nonlinear equations (2.7). When $\boldsymbol{\phi}^{(k)} \in \omega \subset \Omega$ (see the proof of Proposition 2.6), we have a unique solution of the inhomogeneous equations for any $1 \le k \le K$:

$$\phi_{n,m}^{(k)} = -\frac{1}{2} f_{n,m}^{(k)}, \quad (n,m) \in S_M, \qquad \phi_{n,m}^{(k)} = f_{n,m}^{(k)}, \qquad (n,m) \in \mathbb{Z}^2 \setminus S_M,$$

provided that

$$g_{n,m}^{(k)} = -\mathrm{Im}(f_{n,m}^{(k)} \mathrm{e}^{-\mathrm{i}\theta_{n,m}}) = 0, \qquad (n,m) \in S_M, \quad 1 \le k \le K,$$

where $\mathbf{g}^{(k)}$ is defined by (2.18). According to Proposition 2.10, if all $\mathbf{g}^{(k)} = 0$ for $1 \le k \le K-1$, but $(\mathbf{p}_1, \mathbf{g}^{(K)}) \ne 0$, where $\mathbf{p}_1$ is the derivative vector of (3.26) with respect to parameter θ, then the family (3.26) terminates at the K-th order of the Lyapunov–Schmidt reduction.

In the case $M = 1$, when $\mathbf{p}_1 = (0, 1, 0, 1)^{\mathrm{T}}$, we have found from the numerical algorithm that the vector $\mathbf{g}^{(k)}$ is zero for $k = 1, 2, 3, 4, 5$ and non-zero for $k = K = 6$. Moreover, $(\mathbf{p}_1, \mathbf{g}^{(6)}) \ne 0$ for any $\theta \ne \{0, \frac{\pi}{2}, \pi\}$. Similarly, in the case $M = 2$, we have also found that $K = 6$ and $(\mathbf{p}_1, \mathbf{g}^{(6)}) \ne 0$ for any $\theta \ne \{0, \frac{\pi}{2}, \pi\}$. Therefore, our conjecture is confirmed for $M = 1$ and $M = 2$ with the aid of MATLAB.

In the case $M = 3$, we have found that $\mathbf{g}^{(3)}$ is non-zero for any $0 < \theta < \pi$ but it satisfies the constraint $(\mathbf{p}_1, \mathbf{g}^{(3)}) = 0$. Therefore, if the super-symmetric vortex with $M = L = 3$ persists, it must have a non-uniform phase shift across the contour S_3. Our MATLAB-assisted procedure does not allow us to predict whether the family of asymmetric vortices terminates in higher-order reductions $k \ge 4$ if $\mathbf{g}^{(3)} \ne \mathbf{0}$. We will show persistence of a super-symmetric vortex with $M = L = 3$ and termination of the asymmetric vortex (3.26) numerically at the end of Section 5.

3.6. Summary on the persistence of localized modes

Individual results on the persistence of localized modes on the square discrete contour S_M are summarized as follows. Let the localized modes of the nonlinear equations (2.7) be defined by Definitions 2.1–2.3 from the limiting solution $\phi_{n,m}^{(0)}$ in (2.8) and the discrete contour S_M in (2.9). For $M = 1, 2, 3$, there exists a unique (modulo gauge transformation) continuation to the domain $\epsilon \in \mathcal{O}(0)$ of the following families of solutions:

- discrete solitons of family (i) in (3.3);
- symmetric vortices of family (ii) in (3.4);
- zero-parameter asymmetric vortices of family (iv) in (3.6).

Asymmetric vortices of family (iii) in (3.5) cannot be continued to the domain $\epsilon \in \mathcal{O}(0)$ for $M = 1, 2, 3$. In what follows, we consider the stability of persistent localized modes in the time evolution of the discrete NLS equation (2.1).

4. Stability of discrete vortices

The spectral stability of discrete vortices (2.5) with $\mu = 1$ and $\theta_0 = 0$ is studied with the standard linearization:

$$u_{n,m}(t) = \mathrm{e}^{\mathrm{i}(1-4\epsilon)t} \left(\phi_{n,m} + a_{n,m}\mathrm{e}^{\lambda t} + \bar{b}_{n,m}\mathrm{e}^{\bar{\lambda} t} \right), \qquad (n,m) \in \mathbb{Z}^2, \tag{4.1}$$

where $\lambda \in \mathbb{C}$ and $(a_{n,m}, b_{n,m}) \in \mathbb{C}^2$ solve the linear eigenvalue problem on $(n, m) \in \mathbb{Z}^2$:

$$\left(1 - 2|\phi_{n,m}|^2\right) a_{n,m} - \phi_{n,m}^2 b_{n,m} - \epsilon \left(a_{n+1,m} + a_{n-1,m} + a_{n,m+1} + a_{n,m-1}\right) = \mathrm{i}\lambda a_{n,m},$$
$$-\bar{\phi}_{n,m}^2 a_{n,m} + \left(1 - 2|\phi_{n,m}|^2\right) b_{n,m} - \epsilon \left(b_{n+1,m} + b_{n-1,m} + b_{n,m+1} + b_{n,m-1}\right) = -\mathrm{i}\lambda b_{n,m}.$$

The stability problem (4.2) can be formulated in the matrix–vector form:

$$\sigma \mathcal{H} \boldsymbol{\psi} = \mathrm{i}\lambda \boldsymbol{\psi}, \tag{4.2}$$

where $\boldsymbol{\psi} \in \Omega \times \Omega$ consists of 2-blocks of $(a_{n,m}, b_{n,m})^{\mathrm{T}}$, $\mathcal{H}$ is defined by the linearization operator (2.15), and σ consists of 2-by-2 blocks of Pauli matrices σ_3 (σ_3 is the diagonal matrix of $(1, -1)$). The discrete vortex is called spectrally unstable if there exist λ and $\boldsymbol{\psi} \in \Omega \times \Omega$ in the problem (4.2) such that $\mathrm{Re}(\lambda) > 0$. Otherwise, the discrete vortex is called weakly spectrally stable. When the localized mode $\boldsymbol{\phi}(\epsilon)$ is expanded into the Taylor series (2.20), the linearized operator $\mathcal{H}$ is expanded in the corresponding Taylor series:

$$\mathcal{H} = \mathcal{H}^{(0)} + \sum_{k=1}^{\infty} \epsilon^k \mathcal{H}^{(k)}, \tag{4.3}$$

where $\mathcal{H}^{(0)}$ is defined in (2.16), while the first-order and second-order corrections are given by

$$\mathcal{H}_{n,m}^{(1)} = -2 \begin{pmatrix} \bar{\phi}_{n,m}^{(0)} \phi_{n,m}^{(1)} + \phi_{n,m}^{(0)} \bar{\phi}_{n,m}^{(1)} & \phi_{n,m}^{(0)} \phi_{n,m}^{(1)} \\ \bar{\phi}_{n,m}^{(0)} \bar{\phi}_{n,m}^{(1)} & \bar{\phi}_{n,m}^{(0)} \phi_{n,m}^{(1)} + \phi_{n,m}^{(0)} \bar{\phi}_{n,m}^{(1)} \end{pmatrix} - (s_{+1,0} + s_{-1,0} + s_{0,+1} + s_{0,-1}) \begin{pmatrix} 1 & 0 \\ 0 & 1 \end{pmatrix}$$

and

$$\mathcal{H}_{n,m}^{(2)} = -2 \begin{pmatrix} \bar{\phi}_{n,m}^{(0)} \phi_{n,m}^{(2)} + \phi_{n,m}^{(0)} \bar{\phi}_{n,m}^{(2)} & \phi_{n,m}^{(0)} \phi_{n,m}^{(2)} \\ \bar{\phi}_{n,m}^{(0)} \bar{\phi}_{n,m}^{(2)} & \bar{\phi}_{n,m}^{(0)} \phi_{n,m}^{(2)} + \phi_{n,m}^{(0)} \bar{\phi}_{n,m}^{(2)} \end{pmatrix} - \begin{pmatrix} 2|\phi_{n,m}^{(1)}|^2 & \phi_{n,m}^{(1)2} \\ \bar{\phi}_{n,m}^{(1)2} & 2|\phi_{n,m}^{(1)}|^2 \end{pmatrix}.$$

It is clear from the explicit form (2.16) that the spectrum of $\mathcal{H}^{(0)} \boldsymbol{\varphi} = \gamma \boldsymbol{\varphi}$ has exactly N negative eigenvalues $\gamma = -2$, N zero eigenvalues $\gamma = 0$ and infinitely many positive eigenvalues $\gamma = +1$. The negative and zero eigenvalues $\gamma = -2$ and $\gamma = 0$ map to N double zero eigenvalues $\lambda = 0$ in the eigenvalue problem $\sigma \mathcal{H}^{(0)} \boldsymbol{\psi} = \mathrm{i}\lambda \boldsymbol{\psi}$. The positive eigenvalues $\gamma = +1$ map to the infinitely many eigenvalues $\lambda = \pm i$. Since zero eigenvalues of $\sigma \mathcal{H}^{(0)}$ are isolated from the rest of the spectrum, their splitting can be studied through regular perturbation theory. On the other hand, if the localized solution $\phi_{n,m}$ decays sufficiently fast in $(n, m) \in \mathbb{Z}^2$ as $|n| + |m| \to \infty$, the continuous spectral bands of $\sigma \mathcal{H}$ are located on the imaginary axis of λ near the points $\lambda = \pm i$, similarly to the case for $\phi_{n,m} = 0$ for $(n, m) \in \mathbb{Z}^2$ [38]. Therefore, the infinite-dimensional part of the spectrum does not produce any unstable eigenvalues $\mathrm{Re}(\lambda) > 0$ in the stability problem (4.2) with small $\epsilon \in \mathcal{O}(0)$. We shall consider how zero eigenvalues of $\mathcal{H}^{(0)}$ and $\sigma \mathcal{H}^{(0)}$ split as $\epsilon \neq 0$ for the localized modes categorized in Section 3.6.

4.1. Splitting of zero eigenvalues in the first-order reductions

The splitting of zero eigenvalues of $\mathcal{H}$ is related to the Lyapunov–Schmidt reductions of the nonlinear equations (2.14). We show that the same matrix $\mathcal{M}_1$, which gives the Jacobian of the bifurcation functions $\mathbf{g}^{(1)}(\boldsymbol{\theta})$, also defines small eigenvalues of $\mathcal{H}$ that bifurcate from zero eigenvalues of $\mathcal{H}^{(0)}$ in the first-order reductions.

Lemma 4.1. *Let the Jacobian matrix $\mathcal{M}_1$ have eigenvalues $\mu_j^{(1)}$, $1 \leq j \leq N$. The eigenvalue problem $\mathcal{H} \boldsymbol{\varphi} = \gamma \boldsymbol{\varphi}$ has N small eigenvalues γ_j in $\epsilon \in \mathcal{O}(0)$, such that*

$$\lim_{\epsilon \to 0} \frac{\gamma_j}{\epsilon} = \mu_j^{(1)}, \qquad 1 \leq j \leq N. \tag{4.4}$$

Proof. We assume that there exists an analytical solution $\boldsymbol{\phi}(\epsilon)$ of the nonlinear equations (2.14). The Taylor series of $\boldsymbol{\phi}(\epsilon)$ is defined by (2.20). By taking the derivative in ϵ, we rewrite the problem (2.14) in the form

$$\mathcal{H}_p \boldsymbol{\psi}(\epsilon) + \epsilon \mathcal{H}_s \boldsymbol{\psi}(\epsilon) + \mathcal{H}_s \boldsymbol{\phi}(\epsilon) = \mathbf{0}, \qquad \boldsymbol{\psi}(\epsilon) = \boldsymbol{\phi}'(\epsilon), \tag{4.5}$$

where the linearization operator (2.15) is represented as $\mathcal{H} = \mathcal{H}_p + \epsilon \mathcal{H}_s$. Using the series (2.20) and (4.3), we have the linear inhomogeneous equation

$$\mathcal{H}^{(0)} \boldsymbol{\phi}^{(1)} + \mathcal{H}_s \boldsymbol{\phi}^{(0)} = \mathbf{0}. \tag{4.6}$$

Let $\mathbf{e}_j(\boldsymbol{\theta})$, $j = 1, \ldots, N$ be eigenvectors of the kernel of $\mathcal{H}^{(0)}$. Each eigenvector $\mathbf{e}_j(\boldsymbol{\theta})$ contains the only non-zero block $i(\mathrm{e}^{\mathrm{i}\theta_j}, -\mathrm{e}^{-\mathrm{i}\theta_j})^{\mathrm{T}}$ at the j-th position, which corresponds to the node (n, m) on the contour S_M. It is clear that the eigenvectors are orthogonal as follows:

$$(\mathbf{e}_i(\boldsymbol{\theta}), \mathbf{e}_j(\boldsymbol{\theta})) = 2\delta_{i,j}, \qquad 1 \le i, j \le N. \tag{4.7}$$

Let $\hat{\mathbf{e}}_j(\boldsymbol{\theta})$, $j = 1, \ldots, N$ be generalized eigenvectors, such that each eigenvector $\hat{\mathbf{e}}_j(\boldsymbol{\theta})$ contains the only non-zero block $(\mathrm{e}^{\mathrm{i}\theta_j}, \mathrm{e}^{-\mathrm{i}\theta_j})^{\mathrm{T}}$ at the j-th position. Direct computations show that

$$\sigma \mathcal{H}^{(0)} \hat{\mathbf{e}}_j(\boldsymbol{\theta}) = 2i \mathbf{e}_j(\boldsymbol{\theta}), \qquad 1 \le j \le N. \tag{4.8}$$

The limiting solution (2.8) can be represented as follows:

$$\boldsymbol{\phi}^{(0)}(\boldsymbol{\theta}) = \sum_{j=1}^{N} \hat{\mathbf{e}}_j(\boldsymbol{\theta}).$$

By comparing the inhomogeneous equation (4.6) with the definition (2.18) of the bifurcation function $\mathbf{g}(\boldsymbol{\theta})$ and its Taylor series (2.19), we have the correspondence

$$g_j^{(1)}(\boldsymbol{\theta}) = \frac{1}{2}\left(\mathbf{e}_j(\boldsymbol{\theta}), \mathcal{H}_s \boldsymbol{\phi}^{(0)}(\boldsymbol{\theta})\right).$$

Consider a perturbation to a fixed point of $\mathbf{g}^{(1)}(\boldsymbol{\theta}_*) = \mathbf{0}$ in the form $\boldsymbol{\theta} = \boldsymbol{\theta}_* + \epsilon \mathbf{c}$, where $\mathbf{c} = (c_1, c_2, \ldots, c_N)^{\mathrm{T}} \in \mathbb{R}^N$. It is clear that

$$\boldsymbol{\phi}^{(0)}(\boldsymbol{\theta}) = \boldsymbol{\phi}^{(0)} + \epsilon \sum_{i=1}^{N} c_i \mathbf{e}_i + \mathrm{O}(\epsilon^2), \qquad \mathbf{e}_j(\boldsymbol{\theta}) = \mathbf{e}_j - \epsilon c_j \hat{\mathbf{e}}_j + \mathrm{O}(\epsilon^2),$$

where $\boldsymbol{\phi}^{(0)} = \boldsymbol{\phi}^{(0)}(\boldsymbol{\theta}_*)$, $\mathbf{e}_j = \mathbf{e}_j(\boldsymbol{\theta}_*)$, and $\hat{\mathbf{e}}_j = \hat{\mathbf{e}}_j(\boldsymbol{\theta}_*)$. By expanding the bifurcation function $\mathbf{g}^{(1)}(\boldsymbol{\theta})$ near $\boldsymbol{\theta} = \boldsymbol{\theta}_*$, we define the Jacobian matrix $\mathcal{M}_1$:

$$g_j^{(1)}(\boldsymbol{\theta}) = g_j^{(1)} + \epsilon\, (\mathcal{M}_1 \mathbf{c})_j + \mathrm{O}(\epsilon^2),$$

where

$$(\mathcal{M}_1 \mathbf{c})_j = \frac{1}{2} \sum_{i=1}^{n} \left(\mathbf{e}_j, \mathcal{H}_s \mathbf{e}_i\right) c_i - \frac{1}{2} c_j \sum_{i=1}^{N} \left(\hat{\mathbf{e}}_j, \mathcal{H}_s \hat{\mathbf{e}}_i\right). \tag{4.9}$$

On the other hand, the regular perturbation series for small eigenvalues of the problem $\mathcal{H}\boldsymbol{\varphi} = \gamma \boldsymbol{\varphi}$ are defined as follows:

$$\boldsymbol{\varphi} = \boldsymbol{\varphi}^{(0)} + \epsilon \boldsymbol{\varphi}^{(1)} + \epsilon^2 \boldsymbol{\varphi}^{(2)} + \mathrm{O}(\epsilon^3), \qquad \gamma = \epsilon \gamma_1 + \epsilon^2 \gamma_2 + \mathrm{O}(\epsilon^3), \tag{4.10}$$

where $\boldsymbol{\varphi}^{(0)} = \sum_{j=1}^{N} c_j \mathbf{e}_j$, according to the kernel of $\mathcal{H}^{(0)}$. The first-order correction term $\boldsymbol{\varphi}^{(1)}$ satisfies the inhomogeneous equation

$$\mathcal{H}^{(0)} \boldsymbol{\varphi}^{(1)} + \mathcal{H}^{(1)} \boldsymbol{\varphi}^{(0)} = \gamma_1 \boldsymbol{\varphi}^{(0)}. \tag{4.11}$$

Projection to the kernel of $\mathcal{H}^{(0)}$ gives the eigenvalue problem for γ_1:

$$\frac{1}{2}\sum_{i=1}^{N}\left(\mathbf{e}_j, \mathcal{H}^{(1)}\mathbf{e}_i\right) c_i = \gamma_1 c_j. \tag{4.12}$$

By direct computations,

$$-\frac{1}{2}\sum_{i=1}^{N}\left(\hat{\mathbf{e}}_j, \mathcal{H}_s\hat{\mathbf{e}}_i\right) = \cos(\theta_j - \theta_{j+1}) + \cos(\theta_j - \theta_{j-1}) = \frac{1}{2}\sum_{i=1}^{N}\left(\mathbf{e}_j, \mathcal{H}_p^{(1)}\mathbf{e}_i\right),$$

such that the limiting relation (4.4) follows from (4.9) and (4.12) with $\mathcal{H}^{(1)} = \mathcal{H}_p^{(1)} + \mathcal{H}_s$. □

We apply results of Lemma 4.1 to the localized modes categorized in Section 3.6. The numbers of negative, zero and positive eigenvalues of $\mathcal{M}_1$ are denoted as $n(\mathcal{M}_1)$, $z(\mathcal{M}_1)$ and $p(\mathcal{M}_1)$ respectively. They are predicted from Lemmas 3.4–3.6.

For family (i), we compute the parameter A_1 in Lemma 3.4 as $A_1 = (-1)^{N-l}(2l - N)$, where l is defined in Proposition 3.1. By Lemma 3.4, we have $n(\mathcal{M}_1) = N - l - 1$, $z(\mathcal{M}_1) = 1$, and $p(\mathcal{M}_1) = l$ for $0 \le l \le 2M - 1$ and $n(\mathcal{M}_1) = N - l$, $z(\mathcal{M}_1) = 1$, and $p(\mathcal{M}_1) = l - 1$ for $2M + 1 \le l \le 4M$. In the case of super-symmetric solitons for $l = 2M$, by Lemma 3.6, we have $n(\mathcal{M}_1) = 2M - 1$, $z(\mathcal{M}_1) = 2$, and $p(\mathcal{M}_1) = 2M - 1$.

For family (ii), by Lemma 3.5, we have $n(\mathcal{M}_1) = 0$, $z(\mathcal{M}_1) = 1$, and $p(\mathcal{M}_1) = N - 1$ for $1 \le L \le M - 1$ and $n(\mathcal{M}_1) = N - 1$, $z(\mathcal{M}_1) = 1$, and $p(\mathcal{M}_1) = 0$ for $M + 1 \le L \le 2M - 1$, where L is defined in Proposition 3.1. The case of super-symmetric vortices $L = M$ can only be studied in the second-order reductions, since $\mathcal{M}_1 = 0$.

The family (iv) is characterized by the value of $\cos\theta_* \neq 0$, $L \neq M$ and $1 \le n \le N - 1$, $n \neq 2M$, which are specified in Proposition 3.1. The parameter A_1 in Lemma 3.4 is computed as $A_1 = (-1)^{N-n}(\cos\theta_*)^{N-1}(2n - N)$, such that $z(\mathcal{M}_1) = 1$ in all cases. In the case $\cos\theta_* > 0$, by Lemma 3.4, we have $n(\mathcal{M}_1) = N - n - 1$ and $p(\mathcal{M}_1) = n$ for $1 \le n \le 2M - 1$ and $n(\mathcal{M}_1) = N - n$ and $p(\mathcal{M}_1) = n - 1$ for $2M + 1 \le n \le N - 1$. In the opposite case of $\cos\theta_* < 0$, we have $n(\mathcal{M}_1) = n$ and $p(\mathcal{M}_1) = N - n - 1$ for $1 \le n \le 2M - 1$ and $n(\mathcal{M}_1) = n - 1$ and $p(\mathcal{M}_1) = N - n$ for $2M + 1 \le n \le N - 1$.

The splitting of zero eigenvalue of $\mathcal{H}$ is related to splitting of zero eigenvalues of $\sigma\mathcal{H}$ in the stability problem (4.2).

Lemma 4.2. *Let the Jacobian matrix $\mathcal{M}_1$ have eigenvalues $\mu_j^{(1)}$, $1 \le j \le N$. The eigenvalue problem $\sigma\mathcal{H}\boldsymbol{\psi} = \mathrm{i}\lambda\boldsymbol{\psi}$ has N pairs of small eigenvalues λ_j in $\epsilon \in \mathcal{O}(0)$, such that*

$$\lim_{\epsilon\to 0}\frac{\lambda_j^2}{\epsilon} = 2\mu_j^{(1)}, \qquad 1 \le j \le N. \tag{4.13}$$

Proof. The regular perturbation series for small eigenvalues of $\sigma\mathcal{H}$ are defined as follows:

$$\boldsymbol{\psi} = \boldsymbol{\psi}^{(0)} + \sqrt{\epsilon}\boldsymbol{\psi}^{(1)} + \epsilon\boldsymbol{\psi}^{(2)} + \epsilon\sqrt{\epsilon}\boldsymbol{\psi}^{(3)} + \mathrm{O}(\epsilon^2), \qquad \lambda = \sqrt{\epsilon}\lambda_1 + \epsilon\lambda_2 + \epsilon\sqrt{\epsilon}\lambda_3 + \mathrm{O}(\epsilon^2), \tag{4.14}$$

where, due to the relations (4.7) and (4.8), we have

$$\boldsymbol{\psi}^{(0)} = \sum_{j=1}^{N} c_j\mathbf{e}_j, \qquad \boldsymbol{\psi}^{(1)} = \frac{\lambda_1}{2}\sum_{j=1}^{N} c_j\hat{\mathbf{e}}_j, \tag{4.15}$$

according to the kernel and generalized kernel of $\sigma\mathcal{H}^{(0)}$. The second-order correction term $\boldsymbol{\psi}^{(2)}$ satisfies the inhomogeneous equation

$$\mathcal{H}^{(0)}\boldsymbol{\psi}^{(2)} + \mathcal{H}^{(1)}\boldsymbol{\psi}^{(0)} = \mathrm{i}\lambda_1\sigma\boldsymbol{\psi}^{(1)} + \mathrm{i}\lambda_2\sigma\boldsymbol{\psi}^{(0)}. \tag{4.16}$$

Projection to the kernel of $\mathcal{H}^{(0)}$ gives the eigenvalue problem for λ_1:

$$\mathcal{M}_1 \mathbf{c} = \frac{\lambda_1^2}{2} \mathbf{c}, \tag{4.17}$$

where $\mathbf{c} = (c_1, c_2, \ldots, c_N)^{\mathrm{T}}$ and the matrix $\mathcal{M}_1$ is the same as in the eigenvalue problem (4.12). The relation (4.13) follows from (4.17). □

We apply results of Lemma 4.2 to the localized modes of Section 3.6. The numbers of negative, zero and positive eigenvalues of $\mathcal{M}_1$, denoted as $n(\mathcal{M}_1)$, $z(\mathcal{M}_1)$ and $p(\mathcal{M}_1)$, are computed above. Let N_{r}, N_0 and N_{i}^- be the numbers of pairs of real, zero and imaginary eigenvalues of the reduced eigenvalue problem (4.17). The notation N_{i}^- is used for imaginary eigenvalues with negative Krein signature (see [1,36]).

For family (i), we have $N_{\mathrm{i}}^- = N - l - 1$, $N_0 = 1$, and $N_{\mathrm{r}} = l$ for $0 \le l \le 2M - 1$; $N_{\mathrm{i}}^- = N - l - 1$, $N_0 = 2$, and $N_{\mathrm{r}} = l - 1$ for $l = 2M$; and $N_{\mathrm{i}}^- = N - l$, $N_0 = 1$, and $N_{\mathrm{r}} = l - 1$ for $2M + 1 \le l \le N$, where l is defined in Proposition 3.1.

For family (ii), we have $N_{\mathrm{i}}^- = 0$, $N_0 = 1$, and $N_{\mathrm{r}} = N - 1$ for $1 \le L \le M - 1$; $N_{\mathrm{i}}^- = 0$, $N_0 = N$, and $N_{\mathrm{r}} = 0$ for $L = M$; and $N_{\mathrm{i}}^- = N - 1$, $N_0 = 1$, and $N_{\mathrm{r}} = 0$ for $M + 1 \le L \le 2M - 1$, where L is defined in Proposition 3.1.

For family (iv) with $\cos\theta_* > 0$, we have $N_{\mathrm{i}}^- = N - n - 1$, $N_0 = 1$, and $N_{\mathrm{r}} = n$ for $1 \le n \le 2M - 1$ and $N_{\mathrm{i}}^- = N - n$, $N_0 = 1$, and $N_{\mathrm{r}} = n - 1$ for $2M + 1 \le n \le N - 1$. In the opposite case of $\cos\theta_* < 0$, we have $N_{\mathrm{i}}^- = n$, $N_0 = 1$, and $N_{\mathrm{r}} = N - n - 1$ for $1 \le n \le 2M - 1$ and $N_{\mathrm{i}}^- = n - 1$, $N_0 = 1$, and $N_{\mathrm{r}} = N - n$ for $2M + 1 \le n \le N - 1$.

There are several features which are not captured in the first-order reductions. For super-symmetric solitons of family (i), when $l = 2M$ but $a_j \ne (-1)^j a$, the additional zero eigenvalue splits at the second-order reductions, which leads to an additional non-zero eigenvalue of the stability problem (4.2). For symmetric vortices of family (ii), multiple real eigenvalues of the first-order reductions split into the complex domain in the second-order reductions. For super-symmetric vortices of family (ii), when $L = M$, the matrix $\mathcal{M}_1 = 0$, such that non-zero eigenvalues occur in the second-order reductions. Finally, for super-symmetric solitons with $l = 2M$ and $a_j = (-1)^j a$ and super-symmetric vortices with $L = M$, an additional zero eigenvalue bifurcates in the higher-order reductions. These special features of the problem under consideration are addressed in the rest of this section.

4.2. Splitting of zero eigenvalues in the second-order reductions: Super-symmetric solitons

For super-symmetric solitons of family (i), when $l = 2M$ but $a_j \ne (-1)^j a$, the Jacobian matrix $\mathcal{M}_1$ has two zero eigenvalues with eigenvectors $\mathbf{p}_0$ and $\mathbf{p}_1$, but the Jacobian matrix $\mathcal{M}_1 + \epsilon\mathcal{M}_2$ has only one zero eigenvalue with eigenvector $\mathbf{p}_0$. Therefore, the splitting of the zero eigenvalue occurs in the second-order reduction. Extending the regular perturbation series (4.10) to the next order, we find that $\gamma_1 = 0$ for $\mathbf{c} = \mathbf{p}_1$, and

$$\gamma_2 = \frac{(\mathbf{p}_1, \mathcal{M}_2 \mathbf{p}_1)}{(\mathbf{p}_1, \mathbf{p}_1)}.$$

Extending the regular perturbation series (4.14) to the second order, we have find that $\lambda_1^2 = 0$ for $\mathbf{c} = \mathbf{p}_1$, and

$$\lambda_2^2 = 2\frac{(\mathbf{p}_1, \mathcal{M}_2 \mathbf{p}_1)}{(\mathbf{p}_1, \mathbf{p}_1)} = 2\gamma_2.$$

Thus, the splitting of the zero eigenvalue in the second-order reduction is the same as the splitting of zero eigenvalues in the first-order reductions. A positive eigenvalue γ_2 results in a pair of real eigenvalues λ_2, while a negative eigenvalue γ_2 results in a pair of purely imaginary eigenvalues λ_2 of negative Krein signature. This result recovers conclusions of our previous paper [1], where we address the stability of discrete solitons in the one-dimensional NLS lattice.

4.3. Splitting of non-zero eigenvalues in the second-order reductions

We continue the regular perturbation series (4.14) to the second-order reductions. Using explicit solutions for $\boldsymbol{\phi}^{(1)}$, required in $\mathcal{H}^{(1)}$, we compute the explicit solution of the inhomogeneous equation (4.16) subject to the constraint (4.17):

$$\boldsymbol{\psi}^{(2)} = \frac{\lambda_2}{2}\sum_{j=1}^{N} c_j \hat{\mathbf{e}}_j + \frac{1}{2}\sum_{j=1}^{N}(\sin(\theta_{j+1}-\theta_j)c_{j+1} + \sin(\theta_{j-1}-\theta_j)c_{j-1})\hat{\mathbf{e}}_j + \sum_{j=1}^{N} c_j\,(\mathcal{S}_+ + \mathcal{S}_-)\,\mathbf{e}_j, \quad (4.18)$$

where the operators $\mathcal{S}_\pm$ shift elements of $\mathbf{e}_j$ from the node $(n, m) \in S_M$ to the adjacent nodes $(n, m) \in \mathbb{Z}^2 \setminus S_M$, according to enumeration $j = 1, \dots, N$. The third-order correction term $\boldsymbol{\psi}^{(3)}$ satisfies the inhomogeneous equation

$$\mathcal{H}^{(0)}\boldsymbol{\psi}^{(3)} + \mathcal{H}^{(1)}\boldsymbol{\psi}^{(1)} = \mathrm{i}\lambda_1\sigma\boldsymbol{\psi}^{(2)} + \mathrm{i}\lambda_2\sigma\boldsymbol{\psi}^{(1)} + \mathrm{i}\lambda_3\sigma\boldsymbol{\psi}^{(0)}. \quad (4.19)$$

Projection of the combined inhomogeneous problems (4.16) and (4.19) to the kernel of $\mathcal{H}^{(0)}$ gives the extended eigenvalue problem for λ_1 and λ_2:

$$\mathcal{M}_1\mathbf{c} = \frac{\lambda_1^2}{2}\mathbf{c} + \sqrt{\epsilon}\,(\lambda_1\lambda_2\mathbf{c} + \lambda_1\mathcal{L}_1\mathbf{c})\,, \quad (4.20)$$

where the matrix $\mathcal{L}_1$ is defined by

$$(\mathcal{L}_1)_{i,j} = \begin{cases} \sin(\theta_j - \theta_i), & i = j \pm 1, \\ 0, & |i-j| \neq 1 \end{cases} \quad (4.21)$$

subject to the periodic boundary conditions. Let $\mu_j^{(1)}$ be an eigenvalue of the symmetric matrix $\mathcal{M}_1$ with the eigenvector $\mathbf{c}_j$. Then,

$$\lambda_1 = \pm\sqrt{2\mu_j^{(1)}}, \qquad \lambda_2 = -\frac{(\mathbf{c}_j, \mathcal{L}_1\mathbf{c}_j)}{(\mathbf{c}_j, \mathbf{c}_j)}. \quad (4.22)$$

Since the matrix $\mathcal{L}_1$ is skew-symmetric, the second-order correction term λ_2 is purely imaginary, unless $(\mathbf{c}_j, \mathcal{L}_1\mathbf{c}_j) = 0$. For discrete solitons of family (i), we have $\sin(\theta_{j+1}-\theta_j) = 0$, such that $\mathcal{L}_1 = 0$ and $\lambda_2 = 0$. For symmetric vortices of family (ii) with $L \neq M$, the matrix $\mathcal{M}_1$ has double eigenvalues, according to the roots of $\sin^2\frac{\pi n}{N}$ in the explicit solution (3.13). Using the same discrete Fourier transform as in the proof of Lemma 3.5, one can find the values of λ_1 and λ_2 in this case.

Lemma 4.3. *Let all coefficients $a_j = \cos(\theta_{j+1}-\theta_j)$ and $b_j = \sin(\theta_{j+1}-\theta_j)$, $1 \le j \le N$ be the same: $a_j = a$ and $b_j = b$. Eigenvalues of the reduced problem (4.20) are given explicitly:*

$$\lambda_1 = \pm\sqrt{8a}\sin\frac{\pi n}{N}, \qquad \lambda_2 = -2\mathrm{i}b\sin\frac{2\pi n}{N}, \qquad 1 \le n \le N. \quad (4.23)$$

According to Lemma 4.3, all double roots of λ_1 for $n \neq \frac{N}{2}$ and $n \neq N$ split along the imaginary axis in λ_2. When $a > 0$, the splitting occurs in the transverse directions to the real values of λ_1. When $a < 0$, the splitting occurs in the longitudinal directions to the imaginary values of λ_1. The simple roots at $n = \frac{N}{2}$ and $n = N$ are not affected, since $\lambda_2 = 0$ for $n = \frac{N}{2}$ and $n = N$.

4.4. Splitting of zero eigenvalues in the second-order reductions: super-symmetric vortices

We extend results of the regular perturbation series (4.10) and (4.14) to the case $\mathcal{M}_1 = 0$, which occurs for super-symmetric vortices of family (ii) with charge $L = M$. When $\mathcal{M}_1 = 0$, it follows from the problem (4.11) that $\gamma_1 = 0$ and the first-order correction term $\boldsymbol{\varphi}^{(1)}$ has the explicit form

$$\boldsymbol{\varphi}^{(1)} = \frac{1}{2}\sum_{j=1}^{N}(c_{j+1} - c_{j-1})\hat{\mathbf{e}}_j + \sum_{j=1}^{N} c_j\,(\mathcal{S}_+ + \mathcal{S}_-)\,\mathbf{e}_j, \tag{4.24}$$

where the operators $\mathcal{S}_\pm$ are the same as in the formula (4.18). The second-order correction term $\boldsymbol{\varphi}^{(2)}$ satisfies the inhomogeneous equation

$$\mathcal{H}^{(0)}\boldsymbol{\varphi}^{(2)} + \mathcal{H}^{(1)}\boldsymbol{\varphi}^{(1)} + \mathcal{H}^{(2)}\boldsymbol{\varphi}^{(0)} = \gamma_2\boldsymbol{\varphi}^{(0)}. \tag{4.25}$$

Projection to the kernel of $\mathcal{H}^{(0)}$ gives the eigenvalue problem for γ_2:

$$\frac{1}{2}\left(\mathbf{e}_j, \mathcal{H}^{(1)}\boldsymbol{\varphi}^{(1)}\right) + \frac{1}{2}\sum_{i=1}^{N}\left(\mathbf{e}_j, \mathcal{H}^{(2)}\mathbf{e}_i\right)c_i = \gamma_2 c_j. \tag{4.26}$$

By direct computations in the three separate cases $M = 1$, $M = 2$, and $M \geq 3$, one can verify that the matrix on the left-hand side of the eigenvalue problem (4.26) is nothing but the matrix $\mathcal{M}_2$, which is the Jacobian of the nonlinear function $\mathbf{g}^{(2)}(\boldsymbol{\theta})$. Let the numbers of negative, zero and positive eigenvalues of $\mathcal{M}_2$ be denoted as $n(\mathcal{M}_2)$, $z(\mathcal{M}_2)$ and $p(\mathcal{M}_2)$ respectively. For super-symmetric vortices of family (ii), we have computed in Section 3.4 that $n(\mathcal{M}_2) = 0$, $z(\mathcal{M}_2) = 2$ and $p(\mathcal{M}_2) = 2$ for $M = 1$; $n(\mathcal{M}_2) = 1$, $z(\mathcal{M}_2) = 2$ and $p(\mathcal{M}_2) = 5$ for $M = 2$; and $n(\mathcal{M}_2) = 4$, $z(\mathcal{M}_2) = 2$ and $p(\mathcal{M}_2) = 6$ for $M = 3$.

Splitting of zero eigenvalues of $\sigma\mathcal{H}$ is studied with the regular perturbation series (4.14). When $\mathcal{M}_1 = 0$, it follows from the problem (4.16) that $\lambda_1 = 0$, such that the regular perturbation series (4.14) can be re-ordered as follows:

$$\boldsymbol{\psi} = \boldsymbol{\psi}^{(0)} + \epsilon\boldsymbol{\psi}^{(1)} + \epsilon^2\boldsymbol{\psi}^{(2)} + \mathrm{O}(\epsilon^3), \qquad \lambda = \epsilon\lambda_1 + \epsilon^2\lambda_2 + \mathrm{O}(\epsilon^3), \tag{4.27}$$

where

$$\boldsymbol{\psi}^{(0)} = \sum_{j=1}^{N} c_j\mathbf{e}_j, \qquad \boldsymbol{\psi}^{(1)} = \boldsymbol{\varphi}^{(1)} + \frac{\lambda_1}{2}\sum_{j=1}^{N} c_j\hat{\mathbf{e}}_j, \tag{4.28}$$

and $\boldsymbol{\varphi}^{(1)}$ is given by (4.24). The second-order correction term $\boldsymbol{\psi}^{(2)}$ is found from the inhomogeneous equation

$$\mathcal{H}^{(0)}\boldsymbol{\psi}^{(2)} + \mathcal{H}^{(1)}\boldsymbol{\psi}^{(1)} + \mathcal{H}^{(2)}\boldsymbol{\psi}^{(0)} = \mathrm{i}\lambda_1\sigma\boldsymbol{\psi}^{(1)} + \mathrm{i}\lambda_2\sigma\boldsymbol{\psi}^{(0)}. \tag{4.29}$$

Projection to the kernel of $\mathcal{H}^{(0)}$ gives the eigenvalue problem for λ_1:

$$\mathcal{M}_2\mathbf{c} = \lambda_1\mathcal{L}_2\mathbf{c} + \frac{\lambda_1^2}{2}\mathbf{c}, \tag{4.30}$$

where $\mathbf{c} = (c_1, c_2, \ldots, c_N)^{\mathrm{T}}$, the matrix $\mathcal{M}_2$ is the same as in the eigenvalue problem (4.26), and the matrix $\mathcal{L}_2$ follows from the matrix $\mathcal{L}_1$ in the form (4.21) with $\sin(\theta_{j+1} - \theta_j) = 1$, or explicitly:

$$(\mathcal{L}_2)_{i,j} = \begin{cases} +1, & i = j-1 \\ -1, & i = j+1 \\ 0, & |i-j| \neq 1 \end{cases} \tag{4.31}$$

subject to the periodic boundary conditions. Since $\mathcal{M}_2$ is symmetric and $\mathcal{L}_2$ is skew-symmetric, the eigenvalues of the problem (4.30) occur in pairs $(\lambda_1, -\lambda_1)$.

Comparing matrices $\mathcal{M}_2$ in (3.27) and $\mathcal{L}_2$ in (4.31), we understand that $\mathcal{M}_2 = -\frac{1}{2}\mathcal{L}_2^2$. However, the Jacobian matrices $\tilde{\mathcal{M}}_2$ are modified in the case $M = 2$ and $M \geq 3$ by the rank-one and rank-four non-positive matrices

$\Delta\mathcal{M}_2$. As a result, the eigenvalue problem (4.30) can be factorized as follows:

$$\frac{1}{2}\left(\mathcal{L}_2+\lambda_1\right)^2\mathbf{c}=\Delta\mathcal{M}_2\mathbf{c}. \tag{4.32}$$

If $\lambda_1\in\mathbb{R}$, then $(\mathbf{c},\mathcal{L}_2\mathbf{c})=0$ and $(\mathbf{c},\tilde{\mathcal{M}}_2\mathbf{c})>0$. If $\lambda_1\in\mathrm{i}\mathbb{R}$, then either $\mathcal{L}_2\mathbf{c}=-\lambda_1\mathbf{c}$ or $(\mathbf{c},\Delta\mathcal{M}_2\mathbf{c})<0$. In order to associate the Krein signature with purely imaginary eigenvalues λ_1, we consider the energy quadratic form computed at the eigenvector (4.27) for $\lambda\in\mathrm{i}\mathbb{R}$:

$$(\boldsymbol{\psi},\mathcal{H}\boldsymbol{\psi})=\epsilon^2Q_2+\mathrm{O}(\epsilon^3), \tag{4.33}$$

where

$$\begin{aligned}Q_2&=\left(\boldsymbol{\psi}^{(0)},\mathcal{H}^{(2)}\boldsymbol{\psi}^{(0)}+\mathcal{H}^{(1)}\boldsymbol{\psi}^{(1)}+\mathcal{H}^{(0)}\boldsymbol{\psi}^{(2)}\right)+\left(\boldsymbol{\psi}^{(1)},\mathcal{H}^{(1)}\boldsymbol{\psi}^{(0)}+\mathcal{H}^{(0)}\boldsymbol{\psi}^{(1)}\right)\\&=\mathrm{i}\lambda_1\left(\boldsymbol{\psi}^{(0)},\sigma\boldsymbol{\psi}^{(1)}\right)+\mathrm{i}\lambda_1\left(\boldsymbol{\psi}^{(1)},\sigma\boldsymbol{\psi}^{(0)}\right)\\&=\lambda_1\sum_{j=1}^{N}\left(\bar{c}_j\left(c_{j+1}-c_{j-1}\right)-c_j\left(\bar{c}_{j+1}-\bar{c}_{j-1}\right)\right)+2\lambda_1^2\sum_{j=1}^{N}|c_j|^2\\&=2\lambda_1\left(\mathbf{c},(\mathcal{L}_2+\lambda_1)\mathbf{c}\right).\end{aligned}$$

The sign of the energy quadratic form (4.33) coincides with the Krein signature of imaginary eigenvalues λ (see, e.g., [1]). When $\mathcal{L}_2\mathbf{c}=-\lambda_1\mathbf{c}$, eigenvalues $\lambda\in\mathrm{i}\mathbb{R}$ have zero Krein signature at the second-order reductions. When $(\mathbf{c},\Delta\mathcal{M}_2\mathbf{c})<0$, eigenvalues $\lambda\in\mathrm{i}\mathbb{R}$ have negative Krein signature at the second-order reductions.

Computations of eigenvalues of the reduced eigenvalue problem (4.30) are reported in the three distinct cases: $M=1$, $M=2$ and $M=3$.

Case $M=1$: The reduced eigenvalue problem (4.30) takes the form of the difference equation with constant coefficients:

$$-c_{j+2}+2c_j-c_{j-2}=\lambda_1^2c_j+2\lambda_1\left(c_{j+1}-c_{j-1}\right),\qquad 1\le j\le 4M, \tag{4.34}$$

subject to the periodic boundary conditions. By the discrete Fourier transform, the difference equation reduces to the characteristic equation

$$\left(\lambda_1+2\mathrm{i}\sin\frac{\pi n}{2M}\right)^2=0,\qquad 1\le n\le 4M. \tag{4.35}$$

When $M=1$, the reduced eigenvalue problem (4.30) has two eigenvalues of algebraic multiplicity two at $\lambda_1=-2\mathrm{i}$ and $\lambda_1=2i$ and a zero eigenvalue of algebraic multiplicity four. The multiple imaginary eigenvalue $\lambda_1=2\mathrm{i}$ has zero Krein signature, according to the discussion below (4.33).

Case $M=2$: The reduced eigenvalue problem (4.30) takes the form of a system of difference equations with constant coefficients:

$$\begin{aligned}-x_{j+1}+2x_j-x_{j-1}&=\lambda_1^2x_j+2\lambda_1\left(y_j-y_{j-1}\right),\qquad j=1,2,3,4,\\y_{j+1}-2y_{j+2}+y_{j-1}&=\lambda_1^2y_j+2\lambda_1\left(x_{j+1}-x_j\right),\qquad j=1,2,3,4,\end{aligned}$$

where $x_j=c_{2j-1}$ and $y_j=c_{2j}$ subject to the periodic boundary conditions. The characteristic equation for the linear system takes the explicit form

$$\lambda_1^4-2\lambda_1^2\left(1-(-1)^n-8\sin^2\frac{\pi n}{4}\right)+8\sin^2\frac{\pi n}{4}\left(1-(-1)^n-2\sin^2\frac{\pi n}{4}\right)=0,\qquad n=1,2,3,4.$$

The reduced eigenvalue problem (4.30) has three eigenvalues of algebraic multiplicity four at $\lambda_1=-\sqrt{2}\mathrm{i}$, $\lambda_1=\sqrt{2}\mathrm{i}$, and $\lambda_1=0$, and four simple eigenvalues at $\lambda_1=\pm\mathrm{i}\sqrt{\sqrt{80}+8}$ and $\lambda_1=\pm\sqrt{\sqrt{80}-8}$. The multiple imaginary eigenvalue $\lambda_1 = \sqrt{2}\mathrm{i}$ has zero Krein signature, while the simple imaginary eigenvalue $\lambda_1 = \mathrm{i}\sqrt{\sqrt{80}+8}$ has negative Krein signature, according to the discussion below (4.33).

Case $M = 3$: Eigenvalues of the reduced eigenvalue problem (4.30) are computed numerically by using Mathematica. The results are as follows:

$$\lambda_{1,2} = \pm 3.68497\mathrm{i}, \quad \lambda_{3,4} = \lambda_{5,6} = \pm 3.20804\mathrm{i}, \quad \lambda_{7,8} = \pm 2.25068\mathrm{i}, \quad \lambda_{9,10} = \lambda_{11,12} = \pm \mathrm{i},$$
$$\lambda_{13,14} = \lambda_{15,16} = \pm 0.53991, \quad \lambda_{17,18,19,20} = \pm 0.634263 \pm 0.282851\mathrm{i}, \quad \lambda_{21,22,23,24} = 0.$$

Using these computations of eigenvalues, we summarize that the second-order reduced eigenvalue problem (4.30) has no unstable eigenvalues λ when $L = M = 1$; a simple unstable (positive) eigenvalue when $L = M = 2$; two unstable real and two unstable complex eigenvalues when $L = M = 3$.

The destabilization of the super-symmetric vortex with $M = 2$ occurs due to the center node $(2, 2)$, which couples the four even-numbered nodes of the contour S_2 in the second-order reductions. Due to this coupling, the rank-one non-positive matrix $\Delta\mathcal{M}_2$ modifies the Jacobian matrix $\tilde{\mathcal{M}}_2$, which acquires a simple negative eigenvalue, compared to the non-negative matrix $\mathcal{M}_2$. This deformation results in a simple unstable eigenvalue in the reduced eigenvalue problem (4.32).

Similarly, destabilization of the super-symmetric vortex with $M = 3$ occurs due to the coupling of eight nodes of the contour S_3 with four interior corner points $(2, 2)$, $(2, M)$, (M, M), and $(M, 2)$. Due to this coupling, the rank-four non-positive matrix $\Delta\mathcal{M}_2$ leads to four negative eigenvalues in the Jacobian matrix $\tilde{\mathcal{M}}_2$ and to four unstable eigenvalues in the reduced eigenvalue problem (4.32).

We note that if $\Delta\mathcal{M}_2 = 0$ for any $M \geq 1$ (i.e. if all nodes inside the contour S_M would be removed by drilling a hole), the eigenvalues of $\mathcal{M}_2$ would be all positive and the eigenvalues of the reduced problem (4.32) would be all purely imaginary, similarly to in the case $M = 1$. In this case, the eigenvalue problem (4.32) would be solved with the discrete Fourier transform in the form (4.35) for a general $M \geq 1$.

We also note that multiple eigenvalues of zero Krein signatures can split either along the imaginary axis or into the complex domain. When eigenvalues split along the imaginary axis, a multiple eigenvalue of even algebraic multiplicity splits into equal numbers of eigenvalues of positive and negative Krein signatures [39]. We will show numerically in Section 5 that this scenario holds for super-symmetric vortices in the cases $M = 1, 2, 3$.

4.5. Splitting of zero eigenvalues in the higher-order reductions

We study the splitting of zero eigenvalues in higher-order reductions with a modification of the MATLAB-assisted algorithm of Section 3.5.

The regular perturbation series (4.10) for the eigenvalue problem $\mathcal{H}\boldsymbol{\varphi} = \gamma\boldsymbol{\varphi}$ starts with the zero order $\boldsymbol{\varphi}^{(0)} = \sum_{j=1}^{N} c_j \mathbf{e}_j$. We consider the splitting of the double zero eigenvalue of $\mathcal{M}_2$ which corresponds to the eigenvectors $\mathbf{p}_0$ and $\mathbf{p}_1$, where $\mathbf{p}_0 = (1, 1, \ldots, 1, 1)^{\mathrm{T}}$ and $\mathbf{p}_1 = (0, 1, \ldots, 0, 1)^{\mathrm{T}}$. For this purpose, we set $\mathbf{c} = (c_1, \ldots, c_N) = \mathbf{p}_1 + \alpha\mathbf{p}_0$, where α is a parameter. We assume that the splitting occurs at the order K of the higher-order reductions. Once the perturbation series (4.10) is extended up to the order K in the computational domain $(n, m) \in \mathcal{D}(K, M)$, all corrections of the perturbation series can be found from the linear inhomogeneous equations:

$$\mathcal{H}^{(0)}\boldsymbol{\varphi}^{(k)} = -\sum_{m=1}^{k} \mathcal{H}^{(m)}\boldsymbol{\varphi}^{(k-m)}, \qquad 1 \leq k \leq K-1$$

and

$$\mathcal{H}^{(0)}\boldsymbol{\varphi}^{(K)} = -\sum_{m=1}^{K} \mathcal{H}^{(m)}\boldsymbol{\varphi}^{(K-m)} + \gamma_K \boldsymbol{\varphi}^{(0)},$$

where $\gamma = \gamma_K \epsilon^K + O(\epsilon^{K+1})$ is the leading-order approximation for the smallest non-zero eigenvalue of $\mathcal{H}$. The higher-order correction γ_K and the parameter α in the linear superposition are found from the projection formulas, onto the kernel of $\mathcal{H}^{(0)}$.

Applying this algorithm to the super-symmetric vortices with $M = 1$, we have found that $K = 6$, $\alpha = -\frac{1}{2}$, and $\gamma_6 = -16$, such that the zero eigenvalue becomes a small negative eigenvalue for small $\epsilon \neq 0$. In the case $M = 2$, the same algorithm results in the same conclusion with $K = 6$, $\alpha = -\frac{1}{2}$, and $\gamma_6 = -8$. The algorithmic procedure does not work in the case $M = 3$, when the phase difference between two adjacent sites on the discrete contour changes in higher orders of the Lyapunov–Schmidt reductions.

Similarly, we develop the regular perturbation series (4.27) for the eigenvalue problem $\sigma\mathcal{H}\boldsymbol{\psi} = \mathrm{i}\lambda\boldsymbol{\psi}$ starting with the zero order $\boldsymbol{\psi}^{(0)} = \sum_{j=1}^{N} c_j \mathbf{e}_j$ and $\mathbf{c} = \mathbf{p}_1 + \alpha\mathbf{p}_0$, where $\alpha = -\frac{1}{2}$. In the case $M = 1$, we have found that $\lambda_1 = \lambda_2 = 0$ but $\lambda_3 \neq 0$, such that $\lambda_3^2 = -32 = 2\gamma_6$. Therefore, a small negative eigenvalue of $\mathcal{H}$ at $K = 6$ results in a pair of small imaginary eigenvalues of $\sigma\mathcal{H}$ with negative Krein signature, similarly to the standard result of the first-order reductions. The same conclusion was obtained in the case $M = 2$ with $\lambda_3^2 = -16 = 2\gamma_6$. The case $M = 3$ is again omitted from consideration.

4.6. Summary on the stability of localized modes

Individual results on the stability of localized modes on the square discrete contour S_M are summarized as follows. Let families of discrete solitons and vortices be defined in Section 3.6. For $M = 1, 2, 3$, the following solutions are spectrally stable in the domain $\epsilon \in \mathcal{O}(0)$:

- discrete solitons of family (i) with $l = 0$;
- symmetric vortices of family (ii) with the charge $M + 1 \leq L \leq 2M - 1$;
- the symmetric vortex of family (ii) with the charge $L = M = 1$

All other solutions have at least one unstable eigenvalue with $\mathrm{Re}(\lambda) > 0$. We note that stability of discrete solitons of family (i) with $l = 0$ is equivalent to stability of discrete solitons in the one-dimensional NLS lattice, which is proved in our previous paper [1]. When $l = 0$, the limiting solution (2.8) consists of alternating up and down pulses along the contour S_M, similarly to Theorem 3.6 in [1].

5. Numerical results

We perform a numerical analysis (within a prescribed tolerance of 10^{-8}) of the linear stability problem associated with the discrete NLS equation (2.1). We examine discrete vortices in the simplest cases $M = 1$ and $M = 2$. The results are shown in Figs. 2–7 and summarized in Table 1.

In computations of solutions of the problems (2.7) and (4.2), we will use an equivalent renormalization of the problem with the parameter

$$\varepsilon = \frac{\epsilon}{1 - 4\epsilon}.$$

This renormalization is equivalent to keeping the diagonal term $-4\epsilon\phi_{n,m}$ in the right-hand side of the difference equations (2.7). As a result, the discrete solitons and vortices exist in the semi-infinite domain $\varepsilon > 0$ and the finite interval $0 < \epsilon < \frac{1}{4}$. The anti-continuous limit is not affected by the renormalization since $\varepsilon \approx \epsilon$ for small ϵ.

In Figs. 2–7, the top left panel shows the profile of the vortex solution for a specific value of ε by means of contour plots of the real (top left), imaginary (top right), modulus (bottom left) and phase (bottom right) two-dimensional profiles. The squares in each sub-figure show nodes of the discrete lattice $(n, m) \in \mathbb{Z}^2$, where different colors correspond to different values of the plotted quantities, according to the color scheme on the right of each sub-figure.

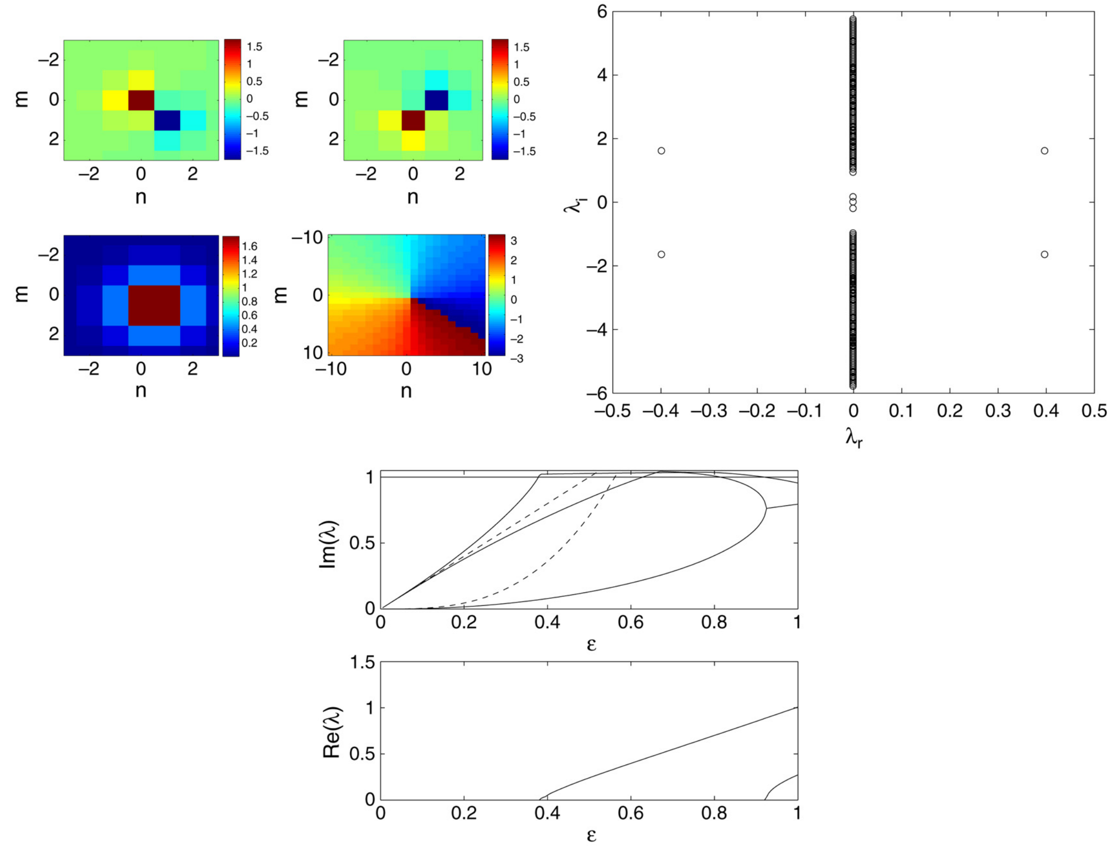

Fig. 2. The (super-symmetric) vortex cell with $L = M = 1$. The top left panel shows the profile of the solution for $\varepsilon = 0.6$. The subplots show the real (top left), imaginary (top right), modulus (bottom left) and phase (bottom right) fields. The top right panel shows the spectral plane (λ_r, λ_i) of the linear eigenvalue problem (4.2). The bottom panel shows the small eigenvalues versus ε (the top subplot shows the imaginary part, while the bottom shows the real part). The solid lines show the numerical results, while the dashed lines show the results of the Lyapunov–Schmidt reductions.

The top right panel shows the complex plane $\lambda = \lambda_r + i\lambda_i$ for the linear eigenvalue problem (4.2) for the same value of ε. The bottom panel shows the dependence of small eigenvalues as a function of ε, obtained via continuation methods from the anti-continuum limit of $\varepsilon = 0$. The solid lines represent numerical results, while the dashed lines show results of the first-order, second-order and sixth-order reductions.

Fig. 2 shows results for the super-symmetric vortex of charge $L = 1$ on the contour S_M with $M = 1$. In the second-order and sixth-order reductions, the stability spectrum of the vortex solution has a pair of imaginary eigenvalues $\lambda \approx \pm i\sqrt{32}\varepsilon^3$ and two pairs of imaginary eigenvalues $\lambda \approx \pm 2\varepsilon i$. The latter pairs split along the imaginary axis beyond the second-order reductions. The larger pair of negative Krein signature leads to a Hamiltonian–Hopf bifurcation for larger values of $\varepsilon \approx 0.38$ upon collision with the continuous spectrum. The smaller pair of positive Krein signature disappears at $\varepsilon \approx 0.66$. The smallest pair of imaginary eigenvalues has negative Krein signature and leads to a Hamiltonian–Hopf bifurcation at $\varepsilon \approx 0.92$ due to collision with another pair of positive Krein signature which bifurcates from the continuous spectrum.

Fig. 3 shows results for the symmetric vortex of charge $L = 1$ on the contour S_M with $M = 2$. There are three double and one simple real unstable eigenvalues in the first-order reductions, but all double eigenvalues split into the complex plane in the second-order reductions. The asymptotic result (4.23) for eigenvalues $\lambda \approx \sqrt{\varepsilon}\lambda_1 + \varepsilon\lambda_2$

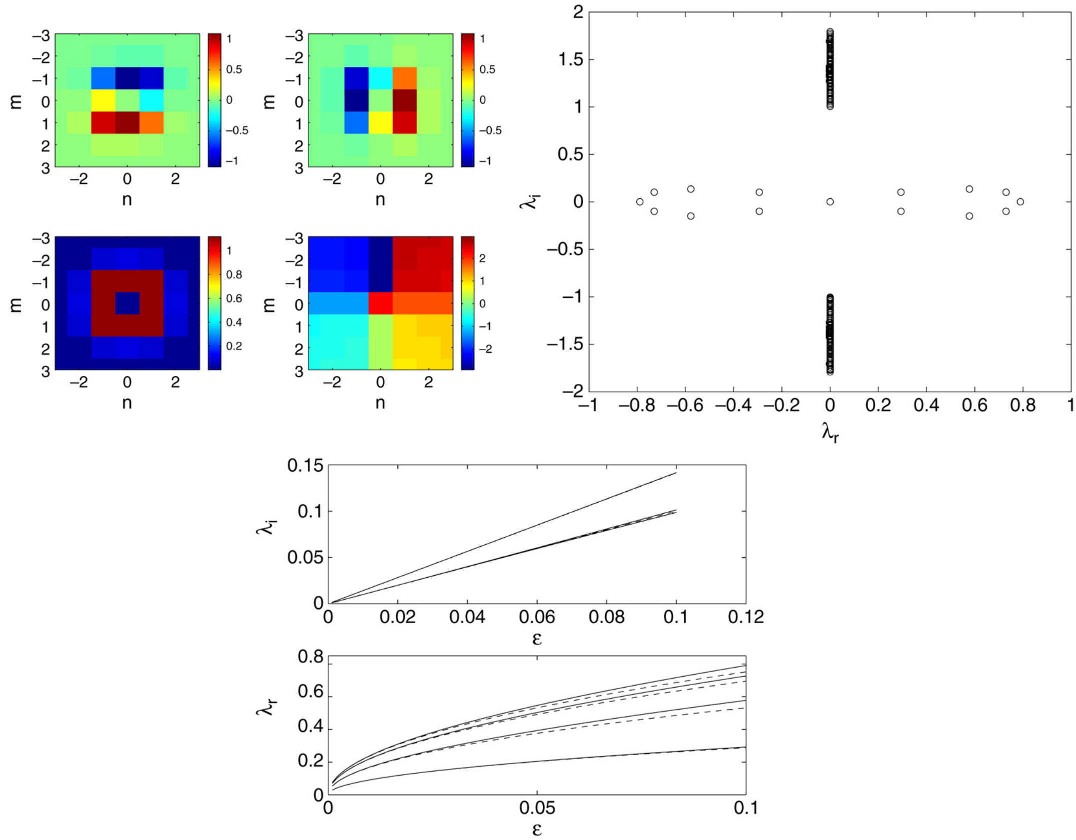

Fig. 3. The symmetric vortex with $L = 1$ and $M = 2$; the top panels show the mode profile (left) and linear stability (right) for $\varepsilon = 0.1$.

with $N = 8$, $a = \cos(\pi/4)$ and $b = \sin(\pi/4)$ is shown in Fig. 3, in very good agreement with numerical results.

Fig. 4 shows results for the super-symmetric vortex with $L = M = 2$. The second-order and sixth-order reductions have a pair of simple real eigenvalues $\lambda \approx \pm\varepsilon\sqrt{\sqrt{80} - 8}$, a pair of simple imaginary eigenvalues $\lambda \approx \pm i\varepsilon\sqrt{\sqrt{80} + 8}$, a pair of simple imaginary eigenvalues $\lambda \approx \pm 4i\varepsilon^3$, and a pair of imaginary eigenvalues of algebraic multiplicity four at $\lambda \approx \pm i\varepsilon\sqrt{2}$. The bottom right panel of Fig. 4 shows the splitting of multiple imaginary eigenvalues beyond the second-order reductions along the imaginary axis and also four subsequent Hamiltonian–Hopf bifurcations for larger values of ε ($\varepsilon \approx 0.23; 0.5; 0.5; 1.45$). The other two pairs of purely imaginary eigenvalues collide with the band edge of the continuous spectrum at $\varepsilon \approx 1.315; 1.395$ and disappear into the continuous spectrum.

Fig. 5 shows results for the symmetric vortex with $L = 3$ and $M = 2$. The first-order reductions predict three pairs of double imaginary eigenvalues, a pair of simple imaginary eigenvalues and a double zero eigenvalue. The double non-zero eigenvalues split in the second-order reductions along the imaginary axis, given by (4.23) with $N = 8$, $a = \cos(3\pi/4)$ and $b = \sin(3\pi/4)$. The seven pairs of imaginary eigenvalues lead to a cascade of seven Hamiltonian–Hopf bifurcations for larger values of ε due to their collisions with the continuous spectrum. The first Hamiltonian–Hopf bifurcation when the symmetric vortex becomes unstable occurs for $\varepsilon \approx 0.096$.

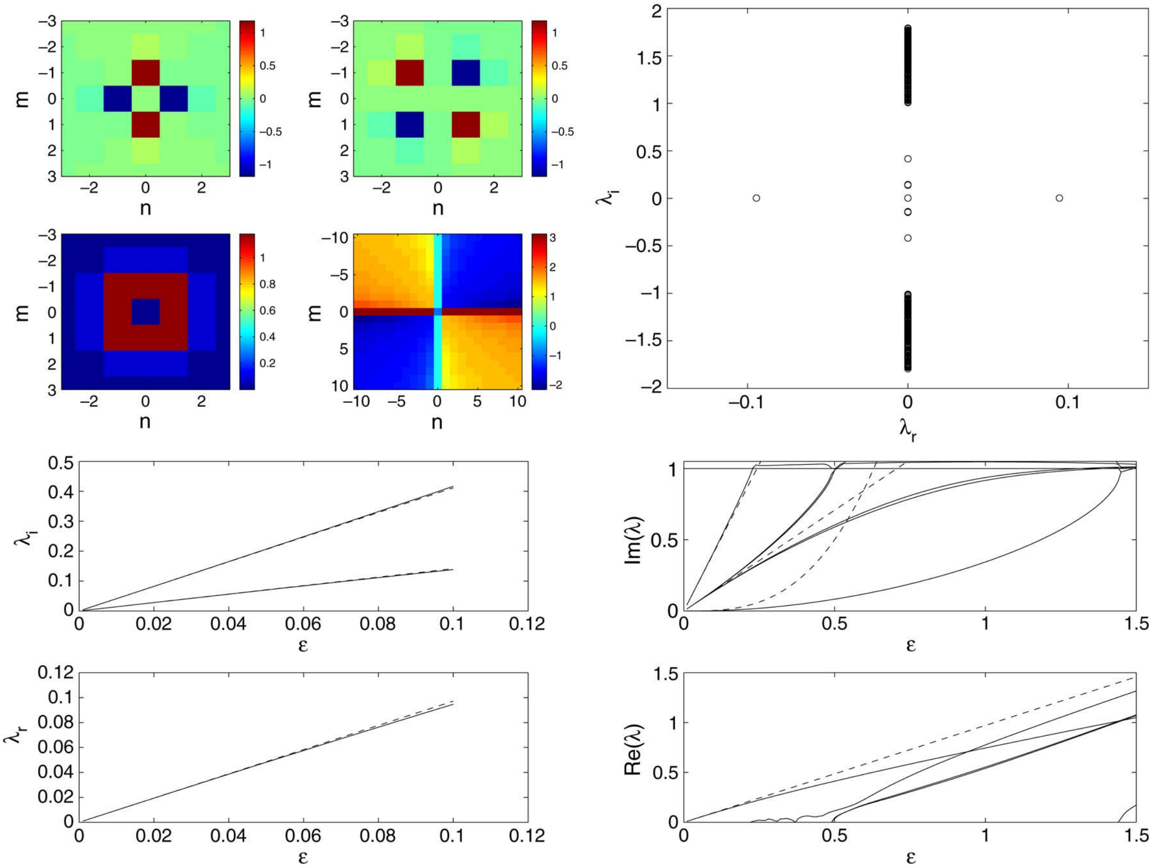

Fig. 4. The super-symmetric vortex with $L = M = 2$; the top panels show the mode profile (left) and linear stability (right) for $\varepsilon = 0.1$. The bottom right panel is an extension of the bottom left panel to larger values of ε.

Zero-parameter asymmetric vortices of family (iv) on the contour S_M with $M = 2$ are shown in Fig. 6 for $L = 1$ and in Fig. 7 for $L = 3$. In the case of Fig. 6, all the phase differences between adjacent sites in the contour are $\pi/6$, except for the last one which is $5\pi/6$, completing a phase trip of 2π for a vortex of topological charge $L = 1$. Eigenvalues of the matrix $\mathcal{M}_1$ in the first-order reductions can be computed numerically as follows: $\mu_1^{(1)} = -1.154$, $\mu_2^{(1)} = 0$, $\mu_3^{(1)} = 0.507$, $\mu_4^{(1)} = 0.784$, $\mu_5^{(1)} = 1.732$, $\mu_6^{(1)} = 2.252$, $\mu_7^{(1)} = 2.957$ and $\mu_8^{(1)} = 3.314$. As a result, the corresponding eigenvalues $\lambda \approx \pm\sqrt{2\mu^{(1)}\varepsilon}$ yield one pair of imaginary eigenvalues and six pairs of real eigenvalues, in agreement with our numerical results. The bottom panel of Fig. 6 shows that two pairs of real eigenvalues collide for $\varepsilon \approx 0.047$ and $\varepsilon \approx 0.057$ and lead to two quartets of eigenvalues.

In the case of Fig. 7, all the phase differences in the contour are $5\pi/6$, except for the last one which is $\pi/6$, resulting in a vortex of topological charge $L = 3$. Eigenvalues of the matrix $\mathcal{M}_1$ are found numerically as follows: $\mu_1^{(1)} = -3.314$, $\mu_2^{(1)} = -2.957$, $\mu_3^{(1)} = -2.252$, $\mu_4^{(1)} = -1.732$, $\mu_5^{(1)} = -0.784$, $\mu_6^{(1)} = -0.507$, $\mu_7^{(1)} = 0$, and $\mu_8^{(1)} = 1.154$. Consequently, this solution has six pairs of imaginary eigenvalues and one pair of real eigenvalues. The first Hamiltonian–Hopf bifurcation occurs for $\varepsilon \approx 0.086$.

At the end of this section, we address the persistence and stability of super-symmetric vortices in the case $M = L = 3$, where our analytical results from Lyapunov–Schmidt reductions have limitations. Numerical computations indicate fast convergence of the iterative procedure to the super-symmetric vortex for $\varepsilon > 0$. Table 2

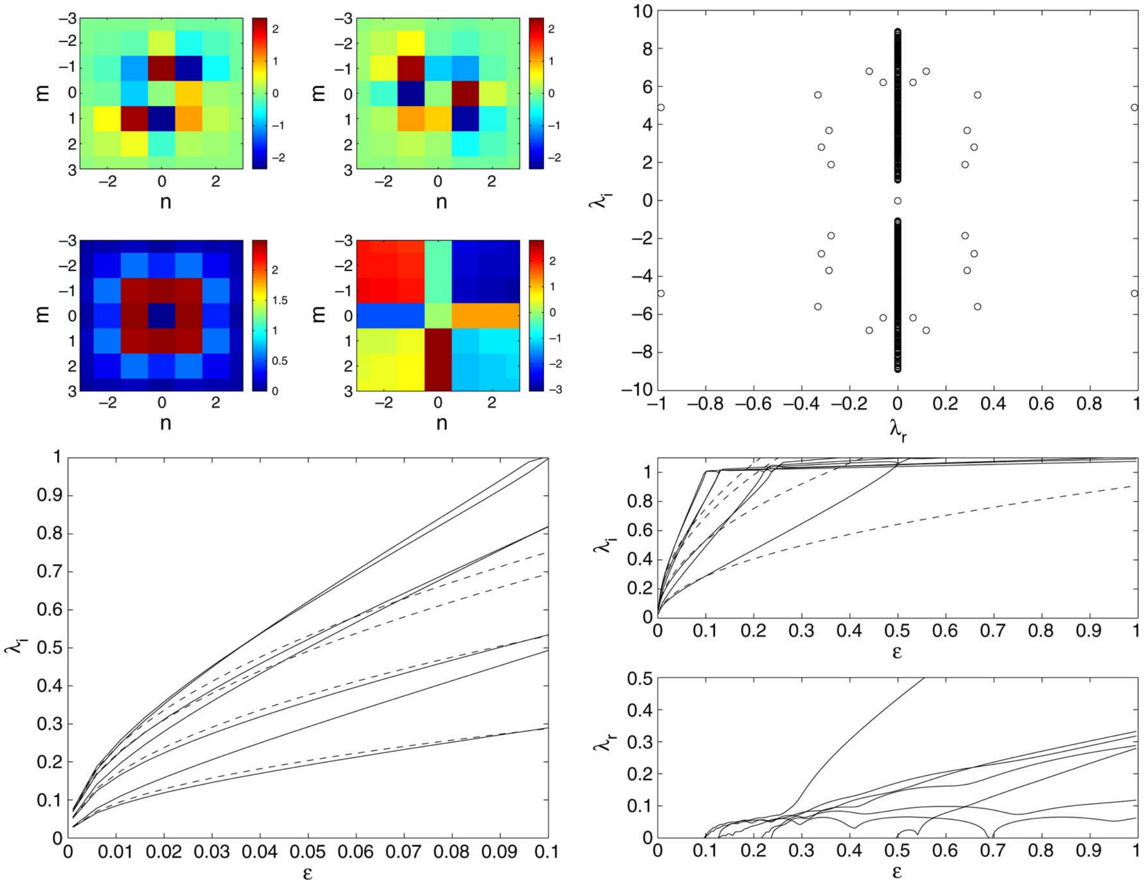

Fig. 5. The symmetric vortex with $L = 3$ and $M = 2$; the top panels show the mode profile (left) and linear stability (right) for $\varepsilon = 0.1$.

Table 2
The phase values of twelve nodes across the discrete contour S_3 in the super-symmetric vortex with $M = L = 3$ for $\varepsilon = 0.01$

$j = 1$	$j = 2$	$j = 3$	$j = 4$	$j = 5$	$j = 6$
0.0012099765	1.5678285580	3.1469803754	4.7135989568	6.2802175384	1.5761840486
$j = 7$	$j = 8$	$j = 9$	$j = 10$	$j = 11$	$j = 12$
3.1428026301	4.7094212116	0.0053877218	1.5720063033	3.1386248848	4.7177767021

shows the values of complex phases θ_j across the discrete contour S_3 for $\varepsilon = 0.01$. It is clear from the Table that the phase differences between two adjacent sites across the discrete contour become slightly different from $\pi/2$, as was noted in the algorithmic computations of the higher-order reductions. Fig. 8 shows the eigenvalues of the discrete spectrum for the super-symmetric vortices with $M = L = 3$ for $\varepsilon = 0.01$. According to our computations of eigenvalues of the second-order reduction, we find four unstable eigenvalues, which include two real and two complex-conjugate eigenvalues. Also, we observe that the additional pair of zero eigenvalues splits slowly from zero in higher-order reductions, which proves our conjecture that the one-parameter family of asymmetric vortices terminates, while the zero-parameter family of super-symmetric vortices persists in the Lyapunov–Schmidt reductions.

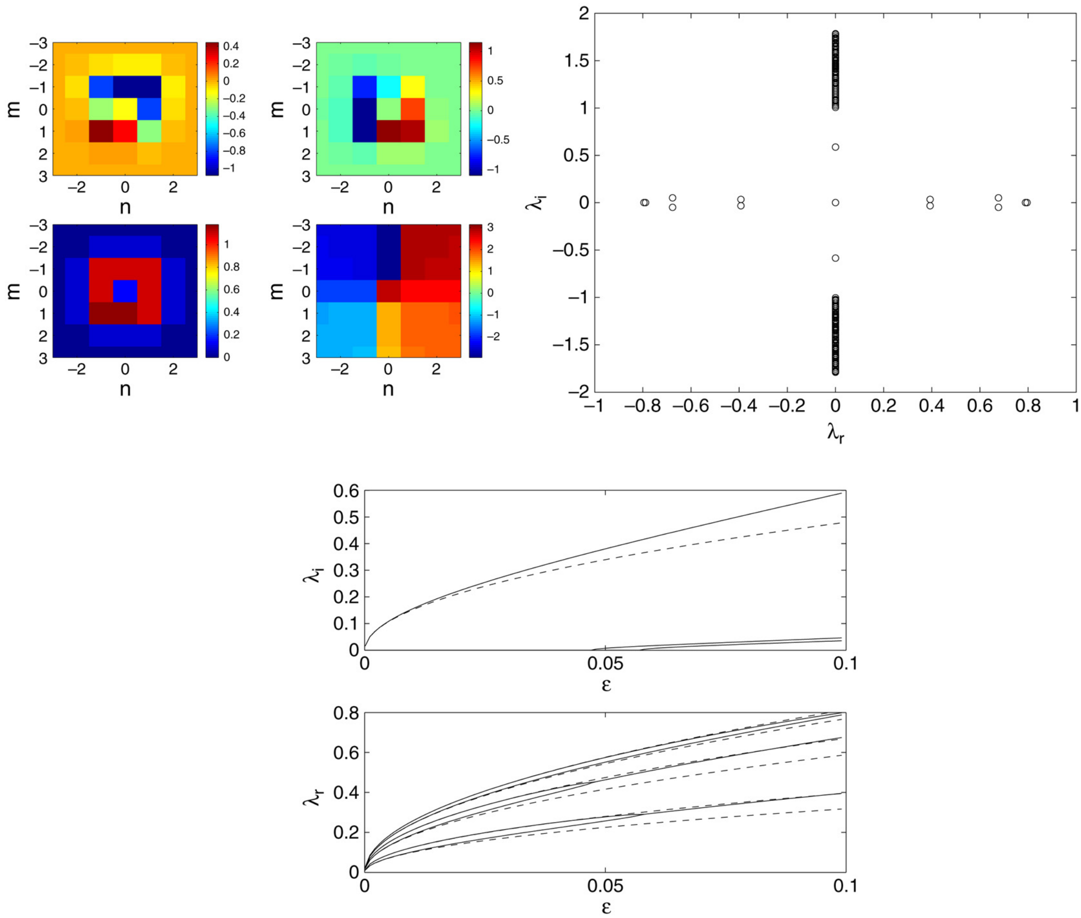

Fig. 6. The asymmetric vortex with $L = 1$ and $M = 2$; the top panels show the mode profile (left) and linear stability (right) for $\varepsilon = 0.1$.

6. Conclusion

In the present work we have developed the mathematical analysis of discrete soliton and vortex solutions of the two-dimensional NLS lattice with small coupling between lattice nodes. These solutions are relevant to recent experimental and numerical studies in the context of nonlinear optics, photonic crystal lattices, soft condensed-matter physics, and Bose–Einstein condensates.

We have examined the persistence of discrete vortices starting from the anti-continuum limit of uncoupled oscillators and continuing towards a finite coupling constant ϵ. We have found persistent families of such solutions that include symmetric and asymmetric vortices. We have ruled out other non-persistent solutions by means of the Lyapunov–Schmidt reduction method. For persistent solutions, we have derived the leading-order asymptotic approximations for small unstable and neutrally stable eigenvalues of the stability problem.

We have applied the results to particular computations of discrete vortices of topological charge $L = 1$, $L = 2$, and $L = 3$ on the discrete square contours S_M with $M = 1$, $M = 2$, and $M = 3$. Besides particular computations collected in Table 1 and Figs. 2–7, these results offer a road map for stability predictions for larger contours, as well as predictions on how to stabilize the discrete vortices. For example, super-symmetric vortices of charge $L = M \geq 2$ can be stabilized by excluding the inner nodes inside the discrete contour S_M.

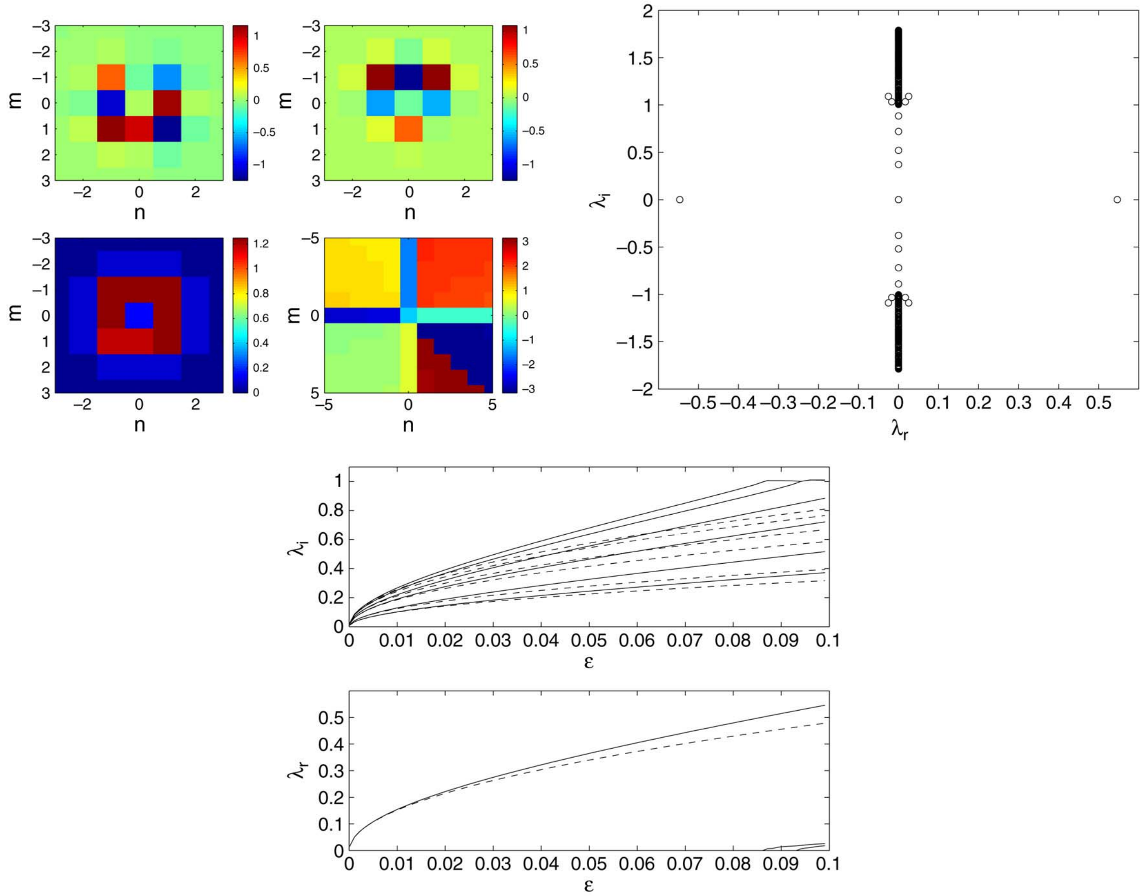

Fig. 7. The asymmetric vortex with $L = 3$ and $M = 2$; the top panels show the mode profile (left) and linear stability (right) for $\varepsilon = 0.1$.

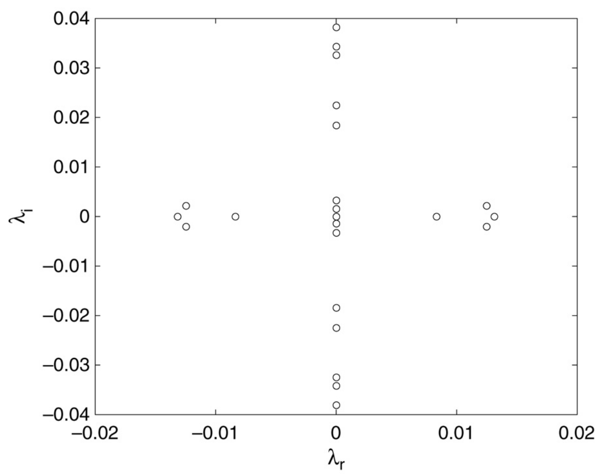

Fig. 8. Eigenvalues of the super-symmetric vortex with $L = 3$ and $M = 3$ for $\varepsilon = 0.01$.

There are remaining open problems for future analytical work. First, it would be nice to extend this analysis to three-dimensional structures, such as the discrete solitons, vortices, or vortex "cubes" (see [26–28]). Second, other types of contours can be studied in the two-dimensional lattice, such as the diagonal square contours which would include the "vortex cross" or the octagon (see [25]). While, conceptually, the methodologies and techniques presented here can be adapted to the problems mentioned above, actual computations of the higher-order Lyapunov–Schmidt reductions become technically involved but can be carried out with symbolic computing software.

Acknowledgements

One of the authors (DEP) thanks R. Kollar and A. Scheel for useful discussions of results of this paper. This work was partially supported by the NSERC and PREA grants for DEP and by the NSF-DMS-0204585, NSF-CAREER, NSF-DMS-0505663 and the Eppley Foundation for Research for PGK.

References

[1] D.E. Pelinovsky, P.G. Kevrekidis, D.J. Frantzeskakis, Stability of discrete solitons in nonlinear Schrödinger equations, Phys. D (2005) Preprint: nlin/0410005. doi:10.1016/j.physd.2005.07.021.
[2] S. Aubry, Breathers in nonlinear lattices: existence, linear stability and quantization, Phys. D 103 (1997) 201–250.
[3] S. Flach, C.R. Willis, Discrete breathers, Phys. Rep. 295 (1998) 181–264.
[4] D. Hennig, G. Tsironis, Wave transmission in nonlinear lattices, Phys. Rep. 307 (1999) 333–432.
[5] P.G. Kevrekidis, K.O. Rasmussen, A.R. Bishop, The discrete nonlinear Schrödinger equation: A survey of recent results, Int. J. Mod. Phys. B 15 (2001) 2833.
[6] V.V. Konotop, V.A. Brazhnyi, Theory of nonlinear matter waves in optical lattices, Mod. Phys. Lett. B 18 (2004) 627–651.
[7] P.G. Kevrekidis, D.J. Frantzeskakis, Pattern forming dynamical instabilities of Bose–Einstein condensates, Mod. Phys. Lett. B 18 (2004) 173–202.
[8] M. Johansson, S. Aubry, Yu.B. Gaididei, P.L. Christiansen, K.O. Rasmussen, Dynamics of breathers in discrete nonlinear Schrödinger models, Phys. D 119 (1998) 115–124.
[9] B.A. Malomed, P.G. Kevrekidis, Discrete vortex solitons, Phys. Rev. E 64 (2001) 026601.
[10] T. Cretegny, S. Aubry, Spatially inhomogeneous time-periodic propagating waves in anharmonic systems, Phys. Rev. B 55 (1997) R11929–R11932.
[11] T. Cretegny, S. Aubry, Patterns of energy flux in periodic solutions of Klein–Gordon lattices, Phys. D 113 (1998) 162–165.
[12] N.K. Efremidis, S. Sears, D.N. Christodoulides, J.W. Fleischer, M. Segev, Discrete solitons in photorefractive optically induced photonic lattices, Phys. Rev. E 66 (2002) 046602.
[13] A.A. Sukhorukov, Yu.S. Kivshar, H.S. Eisenberg, Y. Silberberg, Spatial optical solitons in waveguide arrays, IEEE J. Quantum Electron. 39 (2003) 31–50.
[14] F.S. Cataliotti, S. Burger, C. Fort, P. Maddaloni, F. Minardi, A. Trombettoni, A. Smerzi, M. Inguscio, Josephson junction arrays with Bose–Einstein condensates, Science 293 (2001) 843–846.
[15] F.S. Cataliotti, L. Fallani, F Ferlaino, C. Fort, P. Maddaloni, M. Inguscio, Superfluid current disruption in a chain of weakly coupled Bose–Einstein condensates, New J. Phys. 5 (2003) 71.
[16] J.W. Fleischer, T. Carmon, M. Segev, N.K. Efremidis, D.N. Christodoulides, Observation of discrete solitons in optically induced real time waveguide arrays, Phys. Rev. Lett. 90 (2003) 023902.
[17] H. Martin, E.D. Eugenieva, Z. Chen, D.N. Christodoulides, Discrete solitons and soliton-induced dislocations in partially coherent photonic lattices, Phys. Rev. Lett. 92 (2004) 123902.
[18] J. Yang, I. Makasyuk, A. Bezryadina, Z. Chen, Dipole solitons in optically induced two-dimensional photonic lattices, Opt. Lett. 29 (2004) 1662–1664.
[19] Z. Chen, H. Martin, E.D. Eugenieva, J. Xu, A. Bezryadina, Anisotropic enhancement of discrete diffraction and formation of two-dimensional discrete-soliton trains, Phys. Rev. Lett. 92 (2004) 143902.
[20] Z. Chen, A. Bezryadina, I. Makasyuk, J. Yang, Observation of two-dimensional lattice vector solitons, Opt. Lett. 29 (2004) 1656–1658.
[21] D.N. Neshev, T.J. Alexander, E.A. Ostrovskaya, Yu.S. Kivshar, H. Martin, I. Makasyuk, Z. Chen, Observation of discrete vortex solitons in optically induced photonic lattices, Phys. Rev. Lett. 92 (2004) 123903.
[22] J.W. Fleischer, G. Bartal, O. Cohen, O. Manela, M. Segev, J. Hudock, D.N. Christodoulides, Observation of vortex-ring discrete solitons in 2D photonic lattices, Phys. Rev. Lett. 92 (2004) 123904.

[23] J. Yang, Z. Musslimani, Fundamental and vortex solitons in a two-dimensional optical lattice, Opt. Lett. 28 (2003) 2094–2096.

[24] P.G. Kevrekidis, B.A. Malomed, Z. Chen, D.J. Frantzeskakis, Stable higher-order vortices and quasi-vortices in the discrete nonlinear Schrödinger equation, Phys. Rev. E 70 (2004) 056612.

[25] J. Yang, I. Makasyuk, P.G. Kevrekidis, H. Martin, B.A. Malomed, D.J. Frantzeskakis, Z. Chen, Necklace-like solitons in optically induced photonic lattices, Phys. Rev. Lett. 94 (2005) 113902.

[26] P.G. Kevrekidis, B.A. Malomed, D.J. Frantzeskakis, R. Carretero-González, Three-dimensional solitary waves and vortices in a discrete nonlinear Schrödinger lattice, Phys. Rev. Lett. 93 (2004) 080403.

[27] R. Carretero-González, P.G. Kevrekidis, B.A. Malomed, D.J. Frantzeskakis, Three-dimensional nonlinear lattices: from oblique vortices and octupoles to discrete diamonds and vortex cubes, Phys. Rev. Lett. 94 (2005) 203901.

[28] T.J. Alexander, E.A. Ostrovskaya, A.A. Sukhorukov, Yu.S. Kivshar, Three-dimensional matter-wave vortices in optical lattices. cond-mat/0501590.

[29] T.J. Alexander, A.A. Sukhorukov, Yu.S. Kivshar, Asymmetric vortex solitons in nonlinear periodic lattices, Phys. Rev. Lett. 93 (2004) 063901.

[30] M. Johansson, S. Aubry, Existence and stability of quasiperiodic breathers in the discrete nonlinear Schrödinger equation, Nonlinearity 10 (1997) 1151–1178.

[31] R.S. MacKay, Slow manifolds, in: T. Dauxois, A. Litvak-Hinenzon, R.S. MacKay, A. Spanoudaki (Eds.), Energy Localization and Transfer, World Scientific, Singapore, 2004, pp. 149–192.

[32] R.S. MacKay, S. Aubry, Proof of existence of breathers for time-reversible or Hamiltonian networks of weakly coupled oscillators, Nonlinearity 7 (1994) 1623–1643.

[33] V. Koukouloyannis, R.S. MacKay, Existence and stability of 3-site breathers in a triangular lattice, J. Phys. A: Math. Gen. 38 (2005) 1021–1030.

[34] S.N. Chow, J.K. Hale, Methods of Bifurcation Theory, Springer Verlag, 1982.

[35] M. Golubitsky, D.G. Schaeffer, Singularities and Groups in Bifurcation Theory, vol. 1, Springer Verlag, New York, 1985.

[36] T. Kapitula, P.G. Kevrekidis, Linear stability of perturbed Hamiltonian systems: theory and a case example, J. Phys. A: Math. Gen. 37 (2004) 7509–7526.

[37] B. Sandstede, Stability of multiple-pulse solutions, Trans. Amer. Math. Soc. 350 (1998) 429–472.

[38] H. Levy, F. Lessman, Finite Difference Equations, Dover, New York, 1992.

[39] V. Vougalter, D. Pelinovsky, Eigenvalues of zero energy in the linearized NLS problem, 2005 (preprint).